Appl. Comput. Harmon. Anal. 58 (2022) 60–84

Contents lists available at ScienceDirect

Applied and Computational Harmonic Analysis

www.elsevier.com/locate/acha

Solving phase retrieval with random initial guess is nearly as good as by spectral initialization

Jian-Feng Cai [a,1], Meng Huang [b,*], Dong Li [c], Yang Wang [a,2]

[a] Department of Mathematics, The Hong Kong University of Science and Technology, Clear Water Bay, Kowloon, Hong Kong, China
[b] School of Mathematical Sciences, Beihang University, Beijing, 100191, China
[c] SUSTech International Center for Mathematics and Department of Mathematics, Southern University of Science and Technology, Shenzhen, China

ARTICLE INFO

Article history:
Received 6 October 2020
Received in revised form 8 January 2022
Accepted 14 January 2022
Available online 20 January 2022
Communicated by Hau-Tieng Wu

Keywords:
Phase retrieval
Geometric landscape
Nonconvex
Phaseless measurements

ABSTRACT

The problem of recovering a signal $\boldsymbol{x} \in \mathbb{R}^n$ from a set of magnitude measurements $y_i = |\langle \boldsymbol{a}_i, \boldsymbol{x} \rangle|, \ i = 1, \ldots, m$ is referred as phase retrieval, which has many applications in fields of physical sciences and engineering. In this paper we show that the smoothed amplitude flow based model for phase retrieval has benign geometric structure under the optimal sampling complexity. In particular, we show that when the measurements $\boldsymbol{a}_i \in \mathbb{R}^n$ are Gaussian random vectors and the number of measurements $m \geq Cn$, our smoothed amplitude flow based model has no spurious local minimizers with high probability, i.e., the target solution $\boldsymbol{x}$ is the unique global minimizer (up to a global phase) and the loss function has a negative directional curvature around each saddle point. Due to this benign geometric landscape, the phase retrieval problem can be solved by the gradient descent algorithms without spectral initialization. Numerical experiments show that the gradient descent algorithm with random initialization performs well even comparing with state-of-the-art algorithms with spectral initialization in empirical success rate and convergence speed.

* Corresponding author.
E-mail addresses: jfcai@ust.hk (J.-F. Cai), menghuang@buaa.edu.cn (M. Huang), mpdongli@gmail.com (D. Li), yangwang@ust.hk (Y. Wang).

[1] J. F. Cai was supported in part by Hong Kong Research Grant Council (HKRGC) GRF 16309518, 16309219, 16310620, 16306821.
[2] Y. Wang was supported in part by the Hong Kong Research Grant Council (HKRGC) GRF 16306415 and 16308518.

https://doi.org/10.1016/j.acha.2022.01.002
1063-5203/

1. Introduction

1.1. Background

This paper concerns the well-known phase retrieval problem, which aims to recover the signal $\boldsymbol{x} \in \mathbb{R}^n$ from a series of magnitude-only measurements

$$y_i = |\langle \boldsymbol{a}_i, \boldsymbol{x} \rangle|, \; i = 1, \ldots, m$$

where $\boldsymbol{a}_i \in \mathbb{R}^n, i = 1, \ldots, m$ are Gaussian random vectors and m is the number of measurements. This problem arises in many fields of science and engineering due to the physical limitations of optical detectors which can only record the magnitude of signals while losing the phase information, such as X-ray crystallography [23,32], microscopy [31], astronomy [14], coherent diffractive imaging [12,36] and optics and acoustics [4,5,43] etc. Despite its simple mathematical form, it has been shown that reconstructing a finite-dimensional discrete signal from the magnitude of its Fourier transform is generally an *NP-complete* problem [35].

Many algorithms have been designed to solve the phase retrieval problem. They fall generally into two categories: convex algorithms and non-convex ones. The convex algorithms usually rely on a "matrix-lifting" technique, which lifts the phase retrieval problem into a low rank matrix recovery problem, together with convex relaxation by showing that the matrix recovery problem under some conditions is equivalent to a convex optimization problem. These algorithms include PhaseLift [8,10], PhaseCut [42] etc. It has been shown [8] that PhaseLift can achieve the exact recovery under the optimal sampling complexity with Gaussian random measurements.

Although convex methods have good theoretical guarantees to converge to the true solutions under some special conditions, they tend to be computationally inefficient for large scale problems. By contrast, many non-convex algorithms do not need the lifting step so they operate directly on the lower-dimensional ambient space, making them much more efficient. Early non-convex algorithms were based mostly on alternating projections, e.g. Gerchberg-Saxton [22] and Fineup [17]. The drawback is the lack of theoretical guarantee. Later Netrapalli et al. [33] proposed the AltMinPhase algorithm based on a technique known as *spectral initialization*, and they proved that the algorithm linearly converges to the true solution with $O(n \log^3 n)$ resampling Gaussian random measurements. This work led to further several other non-convex algorithms based on spectral initialization [6,9,11,24,25,41]. They share the common idea of first choosing a good initial guess through spectral initialization, and then solving an optimization model through gradient descent. Two commonly used optimization models are the intensity flow based model

$$\min_{\boldsymbol{z} \in \mathbb{R}^d} \; F(\boldsymbol{z}) = \frac{1}{m} \sum_{j=1}^{m} \left(|\langle \boldsymbol{a}_j, \boldsymbol{z} \rangle|^2 - y_j^2 \right)^2 \tag{1}$$

and the amplitude flow based model

$$\min_{\boldsymbol{z} \in \mathbb{R}^d} \; F(\boldsymbol{z}) = \frac{1}{m} \sum_{j=1}^{m} \left(|\langle \boldsymbol{a}_j, \boldsymbol{z} \rangle| - y_j \right)^2 . \tag{2}$$

Specifically, Candès et al. developed the Wirtinger Flow (WF) [9] method based on (1) and proved that the WF algorithm can achieve linear convergence with $O(n \log n)$ Gaussian random measurements. Lately, Chen and Candès improved the results to $O(n)$ Gaussian random measurements by incorporating a truncation, namely the Truncated Wirtinger Flow (TWF) [11] algorithm. Other methods based on (1) include the Gauss-Newton [19], the trust-region [38], and others. Several algorithms based on the amplitude flow model (2) have also been developed recently, such as the Truncated Amplitude Flow (TAF) algorithm [44], the

Reshaped Wirtinger Flow (RWF) [46] algorithm and the Perturbed Amplitude Flow (PAF) [18] algorithm. All three algorithms above have been shown to linearly converge to the true solution up to a global phase with $O(n)$ Gaussian random measurements. Furthermore, numerical results show that algorithms based on the amplitude flow model (2) tend to outperform algorithms based on model (1). We refer the reader to survey papers [26,36] for accounts of recent developments in the theory, algorithms and applications of phase retrieval.

1.2. Motivation and related work

As we have stated earlier, producing a good initial guess using spectral initialization is a prerequisite for all aforementioned non-convex algorithms with theoretical guarantee. An interesting question is that *Is it possible for those algorithms to achieve successful recovery with a random initialization*?

For intensity-based model (1), the answer is yes. Ju Sun et al. [38] study the global geometry structure of the loss function of (1). They show the loss function $F(\boldsymbol{z})$ does not have any spurious local minima under $O(n \log^3 n)$ Gaussian random measurements. It means that all minimizers are the target signal $\boldsymbol{x}$ up to a global phase and the loss function has a negative directional curvature around each saddle point. Thus any algorithm which can avoid saddle points converges to the true solution with high probability. They also develop a trust-region method to find a global solution with random initialization. To reduce the sampling complexity, it has been shown that the combination of the loss function (1) and an activation function also possesses the benign geometry structure under $O(n)$ Gaussian random measurements [30].

The geometry landscape concept has also been explored in recent years for other applications in signal processing and machine learning. For instance, to understand the surprising phenomenon that why the neural networks can be trained successfully in practice via simple first-order algorithms like gradient descent, several theoretical insights have been provided by analyzing the geometry landscape of over-parameterized shallow neural networks [15,37]. Well-behaved geometry landscapes for optimization, namely all local optimal are also global optimal and the loss function has a negative directional curvature around each saddle point, have been shown to exist more broadly, such as matrix sensing [7,34], tensor decomposition [2,20], dictionary learning [1,3,39], blind deconvolution [29] and matrix completion [21]. Several techniques have been developed to guarantee that the basic gradient optimization algorithms can escape such saddle points efficiently, see e.g. [16,27,28].

1.3. Our contributions

Optimization algorithms based on the amplitude model (2) have been shown to outperform those based on the intensity model (1) [45]. Naturally we may ask whether it is possible to examine the geometric landscape for the amplitude model (2) and develop algorithms similar to the ones in [30,38]. As it turns out, a straightforward approach based on model (2) loss function fails as there will be many local minima regardless how many measurements one take. To remedy this issue, we show that by altering the amplitude model based loss function slightly we are able to obtain to benign geometric landscape for the loss function, thus yielding a fast algorithm that requires only $O(n)$ measurements and no initialization. Furthermore, numerical tests show that the algorithm outperforms several existing algorithms in terms of efficiency.

We now describe our study in more details. Let $\boldsymbol{x} \in \mathbb{R}^n$ be the target signal we want to recover. The measurements we obtain are

$$y_i = |\langle \boldsymbol{a}_i, \boldsymbol{x} \rangle|, \ i = 1, \dots, m$$

where $\boldsymbol{a}_i \in \mathbb{R}^n, i = 1, \dots, m$ are Gaussian random vectors. For the recovery of $\boldsymbol{x}$ we consider the following new loss function $F(\boldsymbol{z})$ given by

$$F(\boldsymbol{z}) = \frac{1}{2m}\sum_{i=1}^{m} y_i^2 \left(\gamma\left(\frac{\boldsymbol{a}_i^\top \boldsymbol{z}}{y_i}\right) - 1\right)^2, \tag{3}$$

where the function $\gamma(t)$ is taken to be

$$\gamma(t) := \begin{cases} |t|, & |t| > \beta; \\ \frac{1}{2\beta}t^2 + \frac{\beta}{2}, & |t| \le \beta, \end{cases} \tag{4}$$

for some constant $0 < \beta \le 1$. Note that the event $\bigcup_{i=1}^m \{\boldsymbol{a}_i^\top \boldsymbol{x} = 0\}$ has zero probability and we may assume that $y_i \neq 0$ for all i. Another practical way is to define $y_i^2\left(\gamma\left(\frac{\boldsymbol{a}_i^\top \boldsymbol{z}}{y_i}\right) - 1\right)^2 = |\boldsymbol{a}_i^\top \boldsymbol{z}|^2$ when $y_i = 0$. A simple observation is that $F(\boldsymbol{z}) = 0$ if and only if $y_i = |\langle \boldsymbol{a}_i, \boldsymbol{x}\rangle|$ for all $i = 1, \ldots, m$, which means any global minimizer of $F(\boldsymbol{z})$ is exactly the true solution $\boldsymbol{x}$ up to a global phase provided $m \ge 2n - 1$ [5,13].

Because $\gamma(t)$ is smoothed from $|t|$ in the amplitude flow model, we shall call our model the *Smoothed Amplitude Flow (SAF)* model. Clearly if we set $\gamma(t) := |t|$ then the loss function is exactly the one of amplitude flow based model given in (2). Unfortunately in this case the loss function does not yield the desired geometric landscape: Regardless how many measurements one take, there will appear multiple local minima. Our new loss function, however, will have the desired property. The main theorem of the paper is the following:

Theorem 1.1. *For any fixed $0 < \beta \le 1/2$, assume $m \ge C\beta^{-2}\log(1/\beta)n$. Let $\boldsymbol{x} \in \mathbb{R}^n$ be nonzero and $\{\boldsymbol{a}_i\}_{i=1}^m$ be i.i.d. random Gaussian vectors, i.e., $\boldsymbol{a}_i \sim \mathcal{N}(0, I_n)$ for all i. Then with probability at least $1 - c'\exp(-c\beta^2 m)$ the loss function $F(\boldsymbol{z})$ given in (3) has no spurious local minima, i.e. all local minima are also global minima and any other critical point is a saddle point with a negative directional curvature. Here C, c and c' are universal positive constants.*

Theorem 1.1 implies that gradient descent with any random initial point will not get stuck in a local minimum. Our result turns out to be not just of theoretical interest. Numerical tests show that this model yields very stable and fast convergence with random initialization and performs as good as or even better than the existing gradient descent methods with spectral initialization.

1.4. Organization

The rest of this paper is organized as follows. In Section 2, we provide an outline of the proof. In Section 3, we break down $\mathbb{R}^n$ into several regions and investigate the geometric property of $F(\boldsymbol{z})$ on each region. In Section 4, we carry out some numerical experiments to demonstrate the effectiveness of our model. Section 5 contains the detailed justification for the technical lemmas presented in Section 3. Finally, the appendix collects some auxiliary lemmas and propositions.

2. Geometric properties of the SAF loss function

Our main theorem is a consequence of the analysis of the geometric landscape of the loss function $F(\boldsymbol{z})$ given in (3). As with [38], we shall decompose $\mathbb{R}^n$ into several regions (not necessarily non-overlapping), on each of which $F(\boldsymbol{z})$ has certain property that will allow us to show that with high probability $F(\boldsymbol{z})$ has no local minimizers other than $\pm\boldsymbol{x}$. Furthermore, we show $F(\boldsymbol{z})$ is strongly convex in a neighborhood of $\pm\boldsymbol{x}$.

Thus our strategy for proving the main result is as follows:

Step 1: Compute the gradient and Hessian of the loss function $F(\boldsymbol{z})$. Since $F(\boldsymbol{z})$ is not 2nd order differentiable we shall consider the directional second derivative of $F(\boldsymbol{z})$. Notice that all these are given by sums of random variables.

Step 2: Apply concentration inequalities such as Bernstein's inequality as well as union bounds to approximate the sums of random variables for a given $\boldsymbol{z}$.

Step 3: Estimate the approximations obtained from concentration inequalities to establish the geometric properties for $F(\boldsymbol{z})$. In particular we shall estimate $\langle \nabla F(\boldsymbol{z}), \boldsymbol{z}\rangle$, $\langle \nabla F(\boldsymbol{z}), \boldsymbol{x}\rangle$, and $D^2_{\boldsymbol{v}} F(\boldsymbol{z})$ where $D^2_{\boldsymbol{v}}$ denotes the directional 2nd order derivative along the direction $\boldsymbol{v}$ of $F(\boldsymbol{z})$.

Because $\gamma(t)$ of (4) is given piecewise, the main difficulty here lies with estimations in step 3. Fortunately, while tedious, they can be done to yield what we will need to prove the theorem.

2.1. Step 1

Note that $F(\boldsymbol{z})$ is continuously differentiable, but it is not 2nd order differentiable, so for the 2nd order derivatives we will resort to directional derivatives. Recall that for a function $g(\boldsymbol{z})$ and any vector $\boldsymbol{v} \neq 0$ in $\mathbb{R}^n$, the *one-side directional derivative of* g at $\boldsymbol{z}$ along the direction $\boldsymbol{v}$ is given by

$$D_{\boldsymbol{v}} g(\boldsymbol{z}) := \lim_{t \to 0^+} \frac{g(\boldsymbol{z} + t\boldsymbol{v}) - g(\boldsymbol{z})}{t}$$

if the limit exists. Furthermore, we denote

$$D^2_{\boldsymbol{v}} g(\boldsymbol{z}) = D_{\boldsymbol{v}}(D_{\boldsymbol{v}} g(\boldsymbol{z}))$$

as the *second order directional derivative of* g at $\boldsymbol{z}$ along the direction $\boldsymbol{v}$. As we shall show, both the gradient $\nabla F(\boldsymbol{z})$ and the $D^2_{\boldsymbol{v}} F(\boldsymbol{z})$ are subexponential random variables in terms of $\boldsymbol{a}^\top \boldsymbol{z}$, $\boldsymbol{a}^\top \boldsymbol{x}$, and $\boldsymbol{a}^\top \boldsymbol{v}$. This enables us to apply concentration inequalities described in Step 2. The details will be given in Section 5.

2.2. Step 2

Concentration inequalities allow us to estimate the sums of random variables so we can estimate them for proving the main result. Also, we will need those inequalities to hold uniformly for *all* $\boldsymbol{z}$ on certain region. This is typically proved by using some δ-nets, and there is no exception here. We shall be dealing with subexponential random variables in this paper and we have:

Lemma 2.1. *Let $g(s, t)$ be a real valued function such that $g(\boldsymbol{a}_i^\top \boldsymbol{z}, \boldsymbol{a}_i^\top \boldsymbol{x})$ is subexponential with subexponential norm $\|g(\boldsymbol{a}_i^\top \boldsymbol{z}, \boldsymbol{a}_i^\top \boldsymbol{x})\|_{\Psi_1} \le \tau$. Assuming that on a compact set Ω we have*

$$\frac{1}{m} \sum_{i=1}^m \left| g(\boldsymbol{a}_i^\top \boldsymbol{z}, \boldsymbol{a}_i^\top \boldsymbol{x}) - g(\boldsymbol{a}_i^\top \boldsymbol{z}_0, \boldsymbol{a}_i^\top \boldsymbol{x}) \right| \le \frac{1}{m} \sum_{i=1}^m K(\boldsymbol{a}_i) |\boldsymbol{a}_i^\top (\boldsymbol{z} - \boldsymbol{z}_0)| \tag{5}$$

for any $\boldsymbol{z}, \boldsymbol{z}_0 \in \Omega$, where $K(\boldsymbol{a}_i)$ is a subgaussian random variable with subgaussian norm η. Then for any $0 < \varepsilon \le \tau$ there exists a universal constant $C > 0$ such that for $m \ge C \max\left(\tau^2/\varepsilon^2, 1/\eta^2, 1\right) \cdot \log(\eta/\varepsilon) \cdot n$ we have

$$\left| \frac{1}{m} \sum_{i=1}^m g(\boldsymbol{a}_i^\top \boldsymbol{z}, \boldsymbol{a}_i^\top \boldsymbol{x}) - \mathbb{E}[g(\boldsymbol{a}_1^\top \boldsymbol{z}, \boldsymbol{a}_1^\top \boldsymbol{x})] \right| \le \varepsilon \tag{6}$$

with probability at least $1 - \exp(-c'(\varepsilon, \tau, \eta) m)$ for all $\boldsymbol{z} \in \Omega$. Here, the constant $c'(\varepsilon, \tau, \eta) := c \cdot \min\left(\varepsilon^2/\tau^2, \eta^2, 1\right)$ for some universal constant $c > 0$.

Proof. We shall give the proof in the Section 5. ∎

2.3. Step 3

To prove the main result we will need to estimate several integrals involving the gradient and directional 2nd order derivatives of $F(\boldsymbol{z})$ for $m \geq Cn$ for some $C > 0$. We shall show that for a given $\boldsymbol{x} \neq 0$, with high probability the Smoothed Amplitude Flow loss function $F(\boldsymbol{z})$ is strictly convex on a small neighborhood of $\pm\boldsymbol{x}$. When $\boldsymbol{z}$ is not too close to being orthogonal to $\boldsymbol{x}$, with high probability $F(\boldsymbol{z})$ has no critical point. Finally, for $\boldsymbol{z}$ close to being orthogonal to $\boldsymbol{x}$, we show that with high probability any critical point is a saddle point with a negative directional curvature. We shall present these in Section 3. Here "with high probability" means there exist constants $c, \delta > 0$ such that the probability is at least $1 - c\exp(-\delta m)$.

3. Proof of the main results

In this section we present the detailed geometric landscape of $F(\boldsymbol{z})$. We first decompose $\mathbb{R}^n$ into several regions (not necessarily non-overlapping). Next, we show $F(\boldsymbol{z})$ is strongly convex in the neighborhood of true solution, and either the gradient doesn't vanish or $F(\boldsymbol{z})$ has a negative directional curvature in other regions.

Since $F(\boldsymbol{z}) = F(-\boldsymbol{z})$, to analyse the SAF model here we may without loss of generality consider solving the SAF model on the half space $\langle \boldsymbol{z}, \boldsymbol{x}\rangle \geq 0$. With this in mind, we denote $\sigma = \sigma(\boldsymbol{z}) := \langle \boldsymbol{z}, \boldsymbol{x}\rangle / \|\boldsymbol{z}\|\|\boldsymbol{x}\| \geq 0$ and $\tau = \tau(\boldsymbol{z}) := \sqrt{1-\sigma^2}$. Then we can decompose $\mathbb{R}^n$ into five regions as shown below.

- $\mathcal{R}_1 := \left\{\boldsymbol{z} \in \mathbb{R}^n : \|\boldsymbol{z}\| \geq \frac{2}{\pi}\left(\tau + \sigma \arctan \frac{\sigma}{\tau}\right) + \delta_0\right\}$,
- $\mathcal{R}_2 := \{\boldsymbol{z} \in \mathbb{R}^n : \varepsilon_0 \leq \|\boldsymbol{z}\| \leq 1 \quad \text{and} \quad \sigma_0 \leq \sigma \leq 1 - \sigma_0\}$,
- $\mathcal{R}_3 := \{\boldsymbol{z} \in \mathbb{R}^n : \varepsilon_0 \leq \|\boldsymbol{z}\| \leq 1 - \varepsilon_0 \quad \text{and} \quad \sigma \geq 1 - \sigma_1\}$,
- $\mathcal{R}_4 := \{\boldsymbol{z} \in \mathbb{R}^n : \|\boldsymbol{z}\| \leq 1 + \delta_1 \quad \text{and} \quad \sigma \leq \sigma_2\} \cup \{\boldsymbol{z} \in \mathbb{R}^n : \|\boldsymbol{z}\| \leq \delta_1\}$,
- $\mathcal{R}_5 := \{\boldsymbol{z} \in \mathbb{R}^n : \operatorname{dist}(\boldsymbol{z}, \boldsymbol{x}) \leq \delta_2\}$,

where $\delta_0, \varepsilon_0, \sigma_0 > 0$ are arbitrary small positive constants and $\delta_1, \delta_2, \sigma_1, \sigma_2$ are some constants which will be specified in our lemmas later. Fig. 1 visualizes the partitioning regions described above and gives the idea of how they cover the whole space.

The properties of $F(\boldsymbol{z})$ over these five regions are summarized in the following five lemmas.

Lemma 3.1. *Assume that $0 < \beta < 1$ and $\|\boldsymbol{x}\| = 1$. For any $\delta_0 > 0$ there exists $\varepsilon_0 > 0$ such that with probability at least $1 - 2\exp(-c\delta_0^2 m)$ for $m \geq C\delta_0^{-2}\log(1/\beta)n$,*

$$\langle \nabla F(\boldsymbol{z}), \boldsymbol{z}\rangle \geq \varepsilon_0 \|\boldsymbol{z}\|^2$$

for all $\|\boldsymbol{z}\| \geq \frac{2}{\pi}\left(\tau + \sigma \arctan \frac{\sigma}{\tau}\right) + \delta_0$, i.e., $\boldsymbol{z} \in \mathcal{R}_1$. Here, C and c are some universal constants.

Lemma 3.2. *Assume that $0 < \beta \leq 1/2$ and $\|\boldsymbol{x}\| = 1$. For any $\varepsilon_0, \sigma_0 > 0$ there exists $\epsilon > 0$ such that with probability at least $1 - 2\exp(-cm)$ for $m \geq C\log(1/\beta)n$, we have $\langle \nabla F(\boldsymbol{z}), \boldsymbol{x}\rangle < -\epsilon$ for all $\boldsymbol{z}$ such that $\varepsilon_0 \leq \|\boldsymbol{z}\| \leq 1$ and $\sigma_0 \leq \sigma \leq 1 - \sigma_0$, i.e., $\boldsymbol{z} \in \mathcal{R}_2$. Here, C and c are some universal constants.*

Lemma 3.3. *Assume that $0 < \beta < 1$ and $\|\boldsymbol{x}\| = 1$. For any $\varepsilon_0 > 0$ there exist $\sigma_1, \epsilon > 0$ such that with probability at least $1 - 2\exp(-cm)$ for $m \geq C\log(1/\beta)n$, we have $\langle \nabla F(\boldsymbol{z}), \boldsymbol{x}\rangle < -\epsilon$ for all $\boldsymbol{z}$ such that $\varepsilon_0 \leq \|\boldsymbol{z}\| \leq 1 - \varepsilon_0$ and $\sigma \geq 1 - \sigma_1$, i.e., $\boldsymbol{z} \in \mathcal{R}_3$. Here, C and c are some universal constants.*

Lemma 3.4. *Assume that $0 < \beta \leq 3/4$ and $\|\boldsymbol{x}\| = 1$. There exist $\sigma_2, \varepsilon_0, \delta_1 > 0$ such that with probability at least $1 - 4\exp(-c\beta^2 m)$ for $m \geq C\beta^{-2}\log(1/\beta)n$ we have $D^2_{\boldsymbol{x}}F(\boldsymbol{z}) < -\varepsilon_0$ for all $\boldsymbol{z}$ such that $\|\boldsymbol{z}\| \leq 1 + \delta_1$ and $\sigma \leq \sigma_2$, as well as all $\boldsymbol{z} \in B_{\delta_1}(0)$. Here, C and c are some universal constants.*

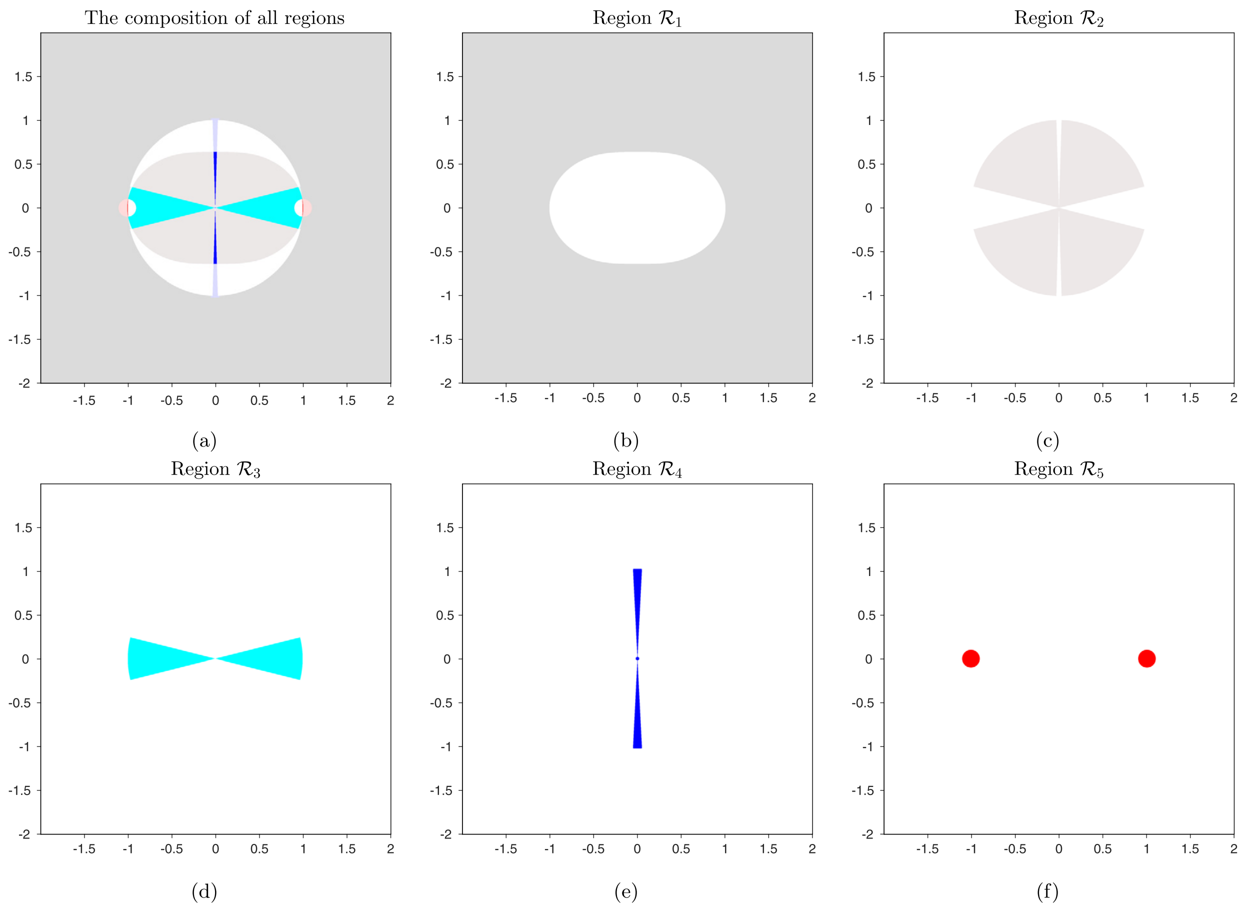

Fig. 1. Partition of $\mathbb{R}^2$: The target signal is $\boldsymbol{x} = [1, 0]$ with constants $\delta_0 = 0.01, \delta_1 = 0.02, \delta_2 = 0.1, \sigma_0 = \sigma_1 = \sigma_2 = 0.05$ and $\varepsilon_0 = 0.1$. (a): The composition of all regions; (b): The region $\mathcal{R}_1$; (c): The region $\mathcal{R}_2$; (d): The region $\mathcal{R}_3$; (e): The region $\mathcal{R}_4$; (f): The region $\mathcal{R}_5$.

Lemma 3.5. *Assume that $0 < \beta < 3/4$ and $\|\boldsymbol{x}\| = 1$. There exists $\delta_2 > 0$ such that with probability at least $1 - 2\exp(-c\beta^2 m)$ for $m \ge C\beta^{-2}\log(1/\beta)n$ we have $D^2_{\boldsymbol{v}} F(\boldsymbol{z}) \ge 0.5$ for all $\boldsymbol{z} \in B_{\delta_2}(\boldsymbol{x})$ and unit vectors $\boldsymbol{v} \in \mathbb{R}^n$. In other words, $F(\boldsymbol{z})$ is strongly convex in $\mathcal{R}_5$. Here, C and c are universal constants.*

The proofs of the above lemmas are given in Section 5. Lemma 3.1, Lemma 3.2 and Lemma 3.3 guarantee the gradient of $F(\boldsymbol{z})$ does not vanish in $\mathcal{R}_1, \mathcal{R}_2$ and $\mathcal{R}_3$, respectively. Thus the critical points of $F(\boldsymbol{z})$ can only occur in $\mathcal{R}_4$ and $\mathcal{R}_5$. However, Lemma 3.4 shows that at any critical point in $\mathcal{R}_4$, $F(\boldsymbol{z})$ has a negative directional curvature. Finally, Lemma 3.5 implies that $F(\boldsymbol{z})$ is strongly convex in $\mathcal{R}_5$. Recognizing that $\nabla F(\boldsymbol{x}) = 0$ and $\boldsymbol{x} \in \mathcal{R}_5$, thus $\boldsymbol{x}$ is the local minimizer. Putting it all together, we can establish Theorem 1.1 as shown below.

Proof of Theorem 1.1. Without loss of generality we shall only examine the region $\sigma \ge 0$, i.e. $\langle \boldsymbol{z}, \boldsymbol{x} \rangle \ge 0$. From Lemma 3.1, Lemma 3.2 and Lemma 3.3, we can see that the constant $\delta_0 > 0$ in region $\mathcal{R}_1$ and the constants $\sigma_0, \varepsilon_0 > 0$ in regions $\mathcal{R}_2$ and $\mathcal{R}_3$ can be sufficiently small. Combining with Lemma 3.4 and Lemma 3.5, it is easy to check that all regions above have covered the whole space to ensure that with probability at least $1 - c' \exp(-c\beta^2 m)$ for $m \gtrsim 1/\beta^2 \log(1/\beta)n$: (i) In a small neighborhood of $\boldsymbol{x}$ the target function $F(\boldsymbol{z})$ is strongly convex with $\boldsymbol{z} = \boldsymbol{x}$ being a minimum. (ii) Everywhere else either the gradient of $F(\boldsymbol{z})$ doesn't vanish or $F(\boldsymbol{z})$ has a negative directional curvature. Thus other than $\boldsymbol{x}$ the target function $F(\boldsymbol{z})$ has no other local minimum.

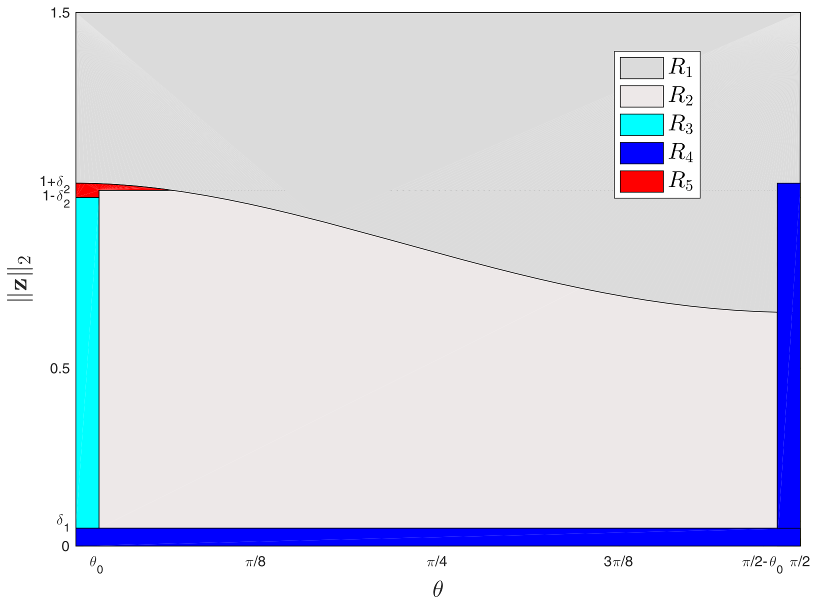

Fig. 2. The partitioning regions for $\mathcal{R}_1, \mathcal{R}_2, \mathcal{R}_3, \mathcal{R}_4$ and $\mathcal{R}_5$ with the norm of $\boldsymbol{z}$ as the function of the angle θ. Here, some regions are overlapping. (For interpretation of the colors in the figure(s), the reader is referred to the web version of this article.)

To illustrate how the regions cover the whole space, let θ be the angle between the vector $\boldsymbol{z}$ and the true solution $\boldsymbol{x}$. Then $0 \leq \theta \leq \pi/2$ and $\sigma = \cos(\theta)$. We can plot the figure of $\|\boldsymbol{z}\|$ with respect to θ as shown in Fig. 2. We can see that all the regions cover the whole space, which proves the theorem. ■

4. Numerical experiments

The SAF model proposed in this paper shows theoretically that any gradient descent algorithm will not get trapped in a local minimum. Here we present numerical experiments to show that the model performs very well with random initial guess.

We use the following vanilla gradient descent algorithm

$$\boldsymbol{z}_{k+1} = \boldsymbol{z}_k - \mu \nabla F(\boldsymbol{z}_k)$$

with a random initial guess to minimize the loss function $F(\boldsymbol{z})$ of SAF. The algorithm procedure is as follows:

Algorithm 1 Gradient descent algorithm based on Smoothed Amplitude Flow (SAF).

Input: Measurement vectors: $\boldsymbol{a}_i \in \mathbb{R}^n, i = 1, \ldots, m$; Observations: $\boldsymbol{y} \in \mathbb{R}^m$; Parameters β; Step size μ; Tolerance $\epsilon > 0$

1: Random initial guess $\boldsymbol{z}_0 \in \mathbb{R}^n$.

2: For $k = 0, 1, 2, \ldots,$ if $\|\nabla F(\boldsymbol{z}_k)\| \geq \epsilon$ do

$$\boldsymbol{z}_{k+1} = \boldsymbol{z}_k - \mu \nabla F(\boldsymbol{z}_k)$$

3: End do

Output: The vector $\boldsymbol{z}_T$.

The performance of our SAF algorithm is conducted via a series of numerical experiments in comparison against WF [9], TWF [11] and TAF [44]. Here, it is worth emphasizing that random initialization is used for our SAF algorithm while all other algorithms have adopted a spectral initialization. Our theoretical results are for real Gaussian case, but the algorithms can be easily adapted to the complex Gaussian case. In our

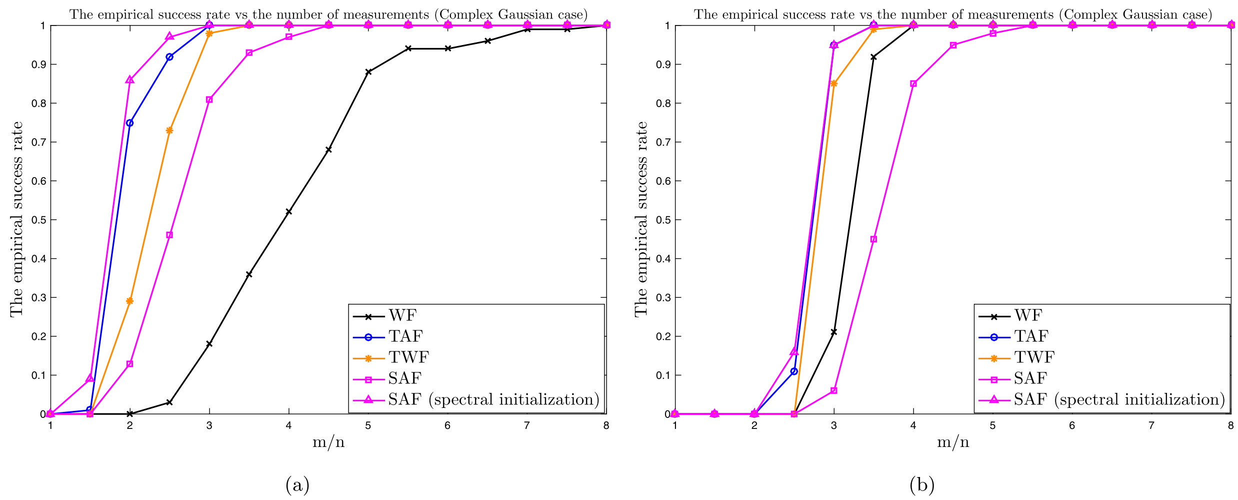

Fig. 3. The empirical success rate for different m/n based on 100 random trails. (a) Success rate for real Gaussian case, (b) success rate for complex Gaussian case.

numerical experiments, the target vector $\boldsymbol{x} \in \mathbb{R}^n$ is chosen randomly from the standard Gaussian distribution and the measurement vectors $\boldsymbol{a}_i$, $i = 1, \dots, m$ are also generated randomly from standard Gaussian distribution. For the real Gaussian case, the signal $\boldsymbol{x} \sim \mathcal{N}(0, I_n)$ and measurement vectors $\boldsymbol{a}_i \sim \mathcal{N}(0, I_n)$ for $i = 1, \dots, m$. For the complex Gaussian case, the signal $\boldsymbol{x} \sim \mathcal{N}(0, I_n) + i\mathcal{N}(0, I_n)$ and measurement vectors $\boldsymbol{a}_i \sim \mathcal{N}(0, I_n/2) + i\mathcal{N}(0, I_n/2)$. For WF, TWF and TAF, we use the code provided in the original papers with suggested parameters.

Example 4.1. In this example, we test the empirical success rate of SAF versus the number of measurements with parameter $\beta = 1/2$. We conduct the experiments for the real and complex Gaussian cases respectively. We choose $n = 128$. The step size $\mu = 0.6$ and the maximum number of iterations is $T = 2000$. For the number of measurements, we vary m within the range $[n, 8n]$. For each m, we run 100 times trials to calculate the success rate. Here, we say a trial to have successfully reconstructed the target signal if the relative error satisfies $\mathrm{dist}(\boldsymbol{z}_T - \boldsymbol{x})/\|\boldsymbol{x}\| \le 10^{-5}$. The results are plotted in Fig. 3. It can be seen that $4.5n$ real Gaussian phaseless measurements or $5.5n$ complex Gaussian phaseless measurements are enough for exactly recovery for SAF with random initialization.

Example 4.2. In this example, we compare the convergence rate of SAF with those of WF, TWF, TAF for real Gaussian and complex Gaussian cases. We choose $n = 128$ and $m = 5n$. The step size $\mu = 0.8$ and parameter $\beta = 1/2$. To show the robustness of our SAF, we also consider the noisy data model $y_i = |\langle \boldsymbol{a}_i, \boldsymbol{x}\rangle| + \eta_i$ where the noise $\eta_i \sim 0.01 \cdot N(0, 1)$. The results are presented in Fig. 4. Since our SAF algorithm chooses a random initial guess according to the standard Gaussian distribution instead of adopting a spectral initialization, it sometimes needs to escape the saddle points with a small number of iterations. Due to its high efficiency to escape the saddle points, it still performs well comparing with state-of-the-art algorithms with spectral initialization.

Example 4.3. In this example, we compare the time elapsed and the iteration needed for WF, TWF, TAF and our SAF to achieve the relative error 10^{-5} and 10^{-10}, respectively. We choose $n = 1000$ with $m = 8n$. The step size $\mu = 0.8$. For the parameter β in our SAF, we consider the case $\beta = 1/2$. We adopt the same spectral initialization method for WF, TWF, TAF and the initial guess is obtained by power method with 50 iterations. We run 50 times trials to calculate the average time elapsed and iteration number for those algorithms. The results are shown in Table 1. The numerical results show that SAF takes around 20 and 40 iterations to escape the saddle points for the real and complex Gaussian cases, respectively. Since there is

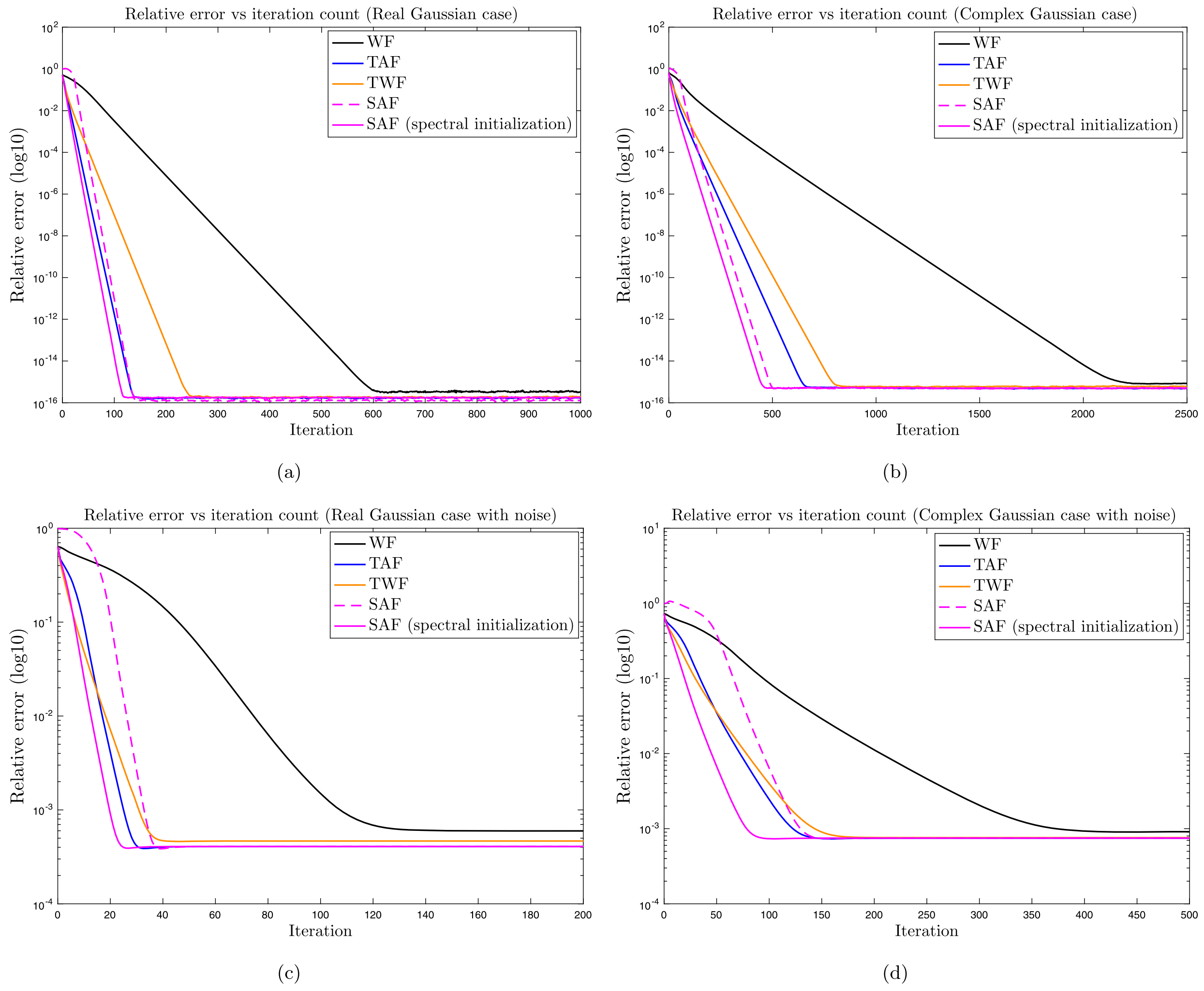

Fig. 4. Relative error versus number of iterations for SAF, WF, TWF, and TAF methods: (a) The noiseless measurements for real Gaussian case; (b) The noiseless measurements for complex Gaussian case; (c) The noisy measurements for real Gaussian case; (d) The noisy measurements for complex Gaussian case.

Table 1
Time Elapsed and Iteration Number among Algorithms on Gaussian Signals with $n = 1000$.

Algorithm	Real Gaussian				Complex Gaussian			
	10^{-5}		10^{-10}		10^{-5}		10^{-10}	
	Iter	Time (s)	Iter	Time (s)	Iter	Time (s)	Iter	Time (s)
SAF	44	**0.1556**	68	**0.2276**	113	**1.3092**	190	**2.3596**
SAF (spectral)	**25**	0.2631	**51**	0.3309	**67**	1.4528	**151**	2.6122
WF	125	4.4214	229	6.3176	304	34.6266	655	86.6993
TAF	29	0.2744	60	0.3515	100	1.7704	211	2.7852
TWF	40	0.3181	87	0.4274	112	1.9808	244	3.7432

no spectral initialization, the high efficiency of escaping saddle points and low computational complexity, the time elapsed of SAF is less than the other methods significantly.

Example 4.4. In this example, we show the performance of SAF with different parameter β in the real Gaussian case. We choose $n = 128$ and the step size $\mu = 0.6$. For SAF with random initialization, we choose $m = 4n$; and for SAF with spectral initialization, we choose $m = 2.5n$. We test the parameter β within the range from 0.1 to 1.0. For each β, we run 100 times trials and calculate the success rate, where a trial is

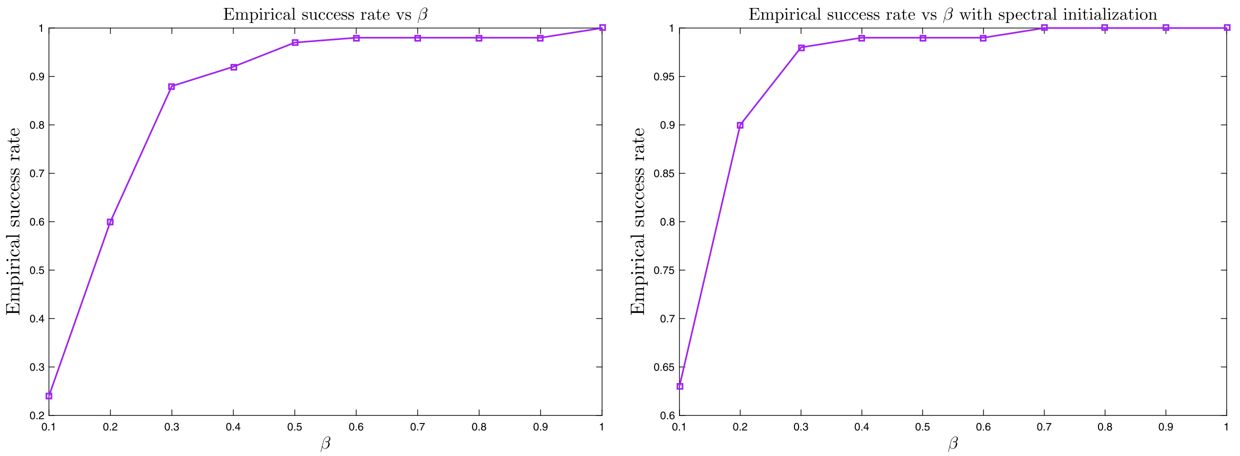

(a) (b)

Fig. 5. Relative error versus the parameter β for SAF: (a) SAF with random initialization under $m = 4n$; (b) SAF with spectral initialization under $m = 2.5n$.

successful if the relative error is less than 10^{-5}. The results are depicted in Fig. 5. From the figures, we can see our SAF has better performance as the parameter β increasing.

5. Proofs of technical results in Section 3

5.1. Notations

In the rest of the paper we shall adopt the following notations and specify some assumptions without loss of generality.

(A1) Without loss of generality, we only consider solving the SAF model on the half space $\langle \boldsymbol{z}, \boldsymbol{x} \rangle \geq 0$. Denote $\sigma = \sigma(\boldsymbol{z}) := \langle \boldsymbol{z}, \boldsymbol{x} \rangle / \|\boldsymbol{z}\| \|\boldsymbol{x}\| \geq 0$ and $\tau = \tau(\boldsymbol{z}) := \sqrt{1 - \sigma^2}$. Furthermore, we shall write

$$\frac{\boldsymbol{z}}{\|\boldsymbol{z}\|} = \sigma \frac{\boldsymbol{x}}{\|\boldsymbol{x}\|} + \tau \boldsymbol{w} \tag{7}$$

where $\boldsymbol{w} \perp \boldsymbol{x}$ and $\|\boldsymbol{w}\| = 1$.

(A2) Denote $\lambda = \beta / \|\boldsymbol{z}\|$. Two quantities that appear often in the paper are $\mu_+ = \mu_+(\lambda, \sigma)$ and $\mu_- = \mu_-(\lambda, \sigma)$ given by

$$\mu_+^2 := 1 + \frac{(\sigma + \lambda)^2}{\tau^2} = \frac{1}{\tau^2}(1 + \lambda^2 + 2\sigma\lambda),$$
$$\mu_-^2 := 1 + \frac{(\sigma - \lambda)^2}{\tau^2} = \frac{1}{\tau^2}(1 + \lambda^2 - 2\sigma\lambda).$$

(A3) We may of course without loss of generality assume that $\|\boldsymbol{x}\| = 1$. Let $\boldsymbol{a} \sim \mathcal{N}(0, I_n)$ be a standard Gaussian vector in $\mathbb{R}^n$. From the orthogonal decomposition $\boldsymbol{z}/\|\boldsymbol{z}\| = \sigma \boldsymbol{x} + \tau \boldsymbol{w}$ in (7), define $U = \boldsymbol{a}^\top \boldsymbol{z}/\|\boldsymbol{z}\|, V = \boldsymbol{a}^\top \boldsymbol{x}$ and $W = \boldsymbol{a}^\top \boldsymbol{w}$. Then $U, V, W \sim \mathcal{N}(0, 1)$ and V, W are independent. Let $A = A(\lambda)$ denote the event

$$A = A(\lambda) := \left\{\boldsymbol{a} : \ |\boldsymbol{a}^\top \boldsymbol{z}| \leq \beta |\boldsymbol{a}^\top \boldsymbol{x}|\right\} = \{\boldsymbol{a} : \ |U| \leq \lambda |V|\}.$$

5.2. Gradient and Hessian of the loss function

For $\boldsymbol{x} \neq 0$ and standard Gaussian random vectors $\{\boldsymbol{a}_i\}_{i=1}^m$, recall that $F(\boldsymbol{z})$ a continuously differentiable function given by

$$F(\boldsymbol{z}) = \frac{1}{2m} \sum_{i=1}^m \left(\gamma\left(\frac{\boldsymbol{a}_i^\top \boldsymbol{z}}{\boldsymbol{a}_i^\top \boldsymbol{x}} \right) - 1 \right)^2 \cdot |\boldsymbol{a}_i^\top \boldsymbol{x}|^2, \tag{8}$$

with

$$\gamma(t) := \begin{cases} |t|, & |t| > \beta; \\ \frac{1}{2\beta} t^2 + \frac{\beta}{2}, & |t| \le \beta. \end{cases}$$

For the convenience, we shall denote

$$f_i(\boldsymbol{z}) = \frac{1}{2} \left(\gamma\left(\frac{\boldsymbol{a}_i^\top \boldsymbol{z}}{\boldsymbol{a}_i^\top \boldsymbol{x}} \right) - 1 \right)^2 \cdot |\boldsymbol{a}_i^\top \boldsymbol{x}|^2$$

and

$$\Psi(u, v) = \frac{1}{2} \left(\gamma\left(\frac{u}{v} \right) - 1 \right)^2 v^2 \quad \text{if} \quad v \neq 0, \quad \text{and} \quad \Psi(u, 0) = \frac{1}{2} u^2. \tag{9}$$

Then the loss function can be denoted as

$$F(\boldsymbol{z}) = \frac{1}{m} \sum_{i=1}^m f_i(\boldsymbol{z}) = \frac{1}{m} \sum_{i=1}^m \Psi(\boldsymbol{a}_i^\top \boldsymbol{z}, \boldsymbol{a}_i^\top \boldsymbol{x}).$$

A simple calculation gives

$$\nabla F(\boldsymbol{z}) = \frac{1}{m} \sum_{i=1}^m \Psi_u(\boldsymbol{a}_i^\top \boldsymbol{z}, \boldsymbol{a}_i^\top \boldsymbol{x}) \boldsymbol{a}_i,$$

where $\Psi_u(u, v)$ is the partial derivative of $\Psi(u, v)$ with respect to u and

$$\Psi_u(u, v) = \left(\gamma\left(\frac{u}{v} \right) - 1 \right) \gamma'\left(\frac{u}{v} \right) v = \begin{cases} \operatorname{sgn}(u)(|u| - |v|), & |u| > \beta |v|; \\ \frac{1}{2\beta^2} \frac{u^3}{v^2} + (\frac{1}{2} - \frac{1}{\beta}) u, & |u| \le \beta |v|. \end{cases} \tag{10}$$

The boundedness and Lipschitz properties of Ψ_u are given in Lemma 6.2.

We next turn to deduce the second order directional derivatives of the target function $F(\boldsymbol{z})$. For any $\boldsymbol{v} \in \mathbb{R}^n$, we have

$$D_{\boldsymbol{v}}^2 F(\boldsymbol{z}) = \frac{1}{m} \sum_{i=1}^m D_{\boldsymbol{v}}^2 f_i(\boldsymbol{z}),$$

where $D_{\boldsymbol{v}}^2$ is the second order directional derivative along the direction $\boldsymbol{v}$. For those points $\boldsymbol{z}$ at which $f_i(\boldsymbol{z})$ has second derivative, it is easy to check that

$$D_{\boldsymbol{v}}^2 f_i(\boldsymbol{z}) = (\boldsymbol{a}_i^\top \boldsymbol{v})^2 + \frac{3}{2\beta^2} \frac{|\boldsymbol{a}_i^\top \boldsymbol{z}|^2}{|\boldsymbol{a}_i^\top \boldsymbol{x}|^2} (\boldsymbol{a}_i^\top \boldsymbol{v})^2 \mathbb{1}_{R_i} - (\frac{1}{2} + \frac{1}{\beta})(\boldsymbol{a}_i^\top \boldsymbol{v})^2 \mathbb{1}_{R_i} \tag{11}$$

with $R_i := \{|\boldsymbol{a}_i^\top \boldsymbol{z}| < \beta|\boldsymbol{a}_i^\top \boldsymbol{x}|\}$. For those points $\boldsymbol{z}$ at which the second derivative of $f_i(\boldsymbol{z})$ does not exist (i.e., $|\boldsymbol{a}_i^\top \boldsymbol{z}| = \beta|\boldsymbol{a}_i^\top \boldsymbol{x}|$), the second order directional derivative along $\boldsymbol{v}$ is well-defined and we have

$$D_{\boldsymbol{v}}^2 f_i(\boldsymbol{z}) = \begin{cases} (\boldsymbol{a}_i^\top \boldsymbol{v})^2, & \text{if} \quad (\boldsymbol{a}_i^\top \boldsymbol{z})(\boldsymbol{a}_i^\top \boldsymbol{v}) > 0; \\ (2 - 1/\beta)(\boldsymbol{a}_i^\top \boldsymbol{v})^2, & \text{if} \quad (\boldsymbol{a}_i^\top \boldsymbol{z})(\boldsymbol{a}_i^\top \boldsymbol{v}) \le 0. \end{cases}$$

In summary, for any $\boldsymbol{z}$ the second order directional derivative of $f_i(\boldsymbol{z})$ along $\boldsymbol{v}$ is

$$D_{\boldsymbol{v}}^2 f_i(\boldsymbol{z}) = (\boldsymbol{a}_i^\top \boldsymbol{v})^2 + \frac{3}{2\beta^2}\frac{|\boldsymbol{a}_i^\top \boldsymbol{z}|^2}{|\boldsymbol{a}_i^\top \boldsymbol{x}|^2} \cdot |\boldsymbol{a}_i^\top \boldsymbol{v}|^2 \mathbb{1}_{R_i} - (\frac{1}{2} + \frac{1}{\beta})(\boldsymbol{a}_i^\top \boldsymbol{v})^2 \mathbb{1}_{R_i} + \Gamma_i(\boldsymbol{z}, \boldsymbol{v}) \tag{12}$$

with

$$\Gamma_i(\boldsymbol{z}, \boldsymbol{v}) := (q_i - 1)\,(\boldsymbol{a}_i^\top \boldsymbol{v})^2 \mathbb{1}_{\{|\boldsymbol{a}_i^\top \boldsymbol{z}| = \beta|\boldsymbol{a}_i^\top \boldsymbol{x}|\}} \le 0.$$

Here, $q_i = 1$ if $(\boldsymbol{a}_i^\top \boldsymbol{z})(\boldsymbol{a}_i^\top \boldsymbol{v}) > 0$ and $q_i = 2 - 1/\beta$ if $(\boldsymbol{a}_i^\top \boldsymbol{z})(\boldsymbol{a}_i^\top \boldsymbol{v}) \le 0$.

5.3. Proof of Lemma 2.1

Proof. For any fixed $\boldsymbol{z}_0 \in \Omega$, the terms $g(\boldsymbol{a}_i^\top \boldsymbol{z}_0, \boldsymbol{a}_i^\top \boldsymbol{x})$ are subexponential random variables with subexponential norm τ. By Lemma 6.1, with probability at least $1 - 2\exp\left(-c\varepsilon^2 m/\tau^2\right)$ it holds

$$\left|\frac{1}{m}\sum_{i=1}^m g(\boldsymbol{a}_i^\top \boldsymbol{z}_0, \boldsymbol{a}_i^\top \boldsymbol{x}) - \mathbb{E}[g(\boldsymbol{a}_1^\top \boldsymbol{z}_0, \boldsymbol{a}_1^\top \boldsymbol{x})]\right| \le \frac{\varepsilon}{3} \tag{13}$$

for any $\varepsilon \le \tau$. To obtain the union bound for all $\boldsymbol{z} \in \Omega$ we need a (standard) covering argument. Since Ω is compact, we can construct a δ_0-net $\mathcal{N}$ with $\mathrm{Card}(\mathcal{N}) \le \exp(n\log(3R/\delta_0))$ (R is the radius of Ω) such that

$$\mathcal{N} \subset \Omega \subset \bigcup_{\tilde{\boldsymbol{z}} \in \mathcal{N}} B(\tilde{\boldsymbol{z}}, \delta_0).$$

Here $\delta_0 > 0$ is a constant which will be taken sufficiently small. The needed smallness will be specified later. By using the above construction, for any $\boldsymbol{z} \in \Omega$, we can find a vector $\boldsymbol{z}_0 \in \mathcal{N}$ such that $\|\boldsymbol{z} - \boldsymbol{z}_0\| \le \delta_0$. Since $K(\boldsymbol{a}_i)$ are subgaussian random variables with subgaussian norm η, Lemma 6.1 implies that with probability at least $1 - 2\exp\left(-cm\min(\delta_1^2/\eta^2, \delta_1/\eta)\right)$ it holds

$$\frac{1}{m}\sum_{i=1}^m K(\boldsymbol{a}_i)^2 \le \mathbb{E}K(\boldsymbol{a}_1)^2 + \delta_1 \le \eta^2 + \delta_1,$$

where $\delta_1 > 0$ will be taken sufficiently small. On the other hand, we have

$$\begin{aligned} &\left|\frac{1}{m}\sum_{i=1}^m g(\boldsymbol{a}_i^\top \boldsymbol{z}, \boldsymbol{a}_i^\top \boldsymbol{x}) - \frac{1}{m}\sum_{i=1}^m g(\boldsymbol{a}_i^\top \boldsymbol{z}_0, \boldsymbol{a}_i^\top \boldsymbol{x})\right| \\ &\le \frac{1}{m}\sum_{i=1}^m K(\boldsymbol{a}_i)|\boldsymbol{a}_i^\top(\boldsymbol{z} - \boldsymbol{z}_0)| \\ &\le \sqrt{\frac{1}{m}\sum_{i=1}^m K(\boldsymbol{a}_i)^2} \cdot \sqrt{\frac{1}{m}\sum_{i=1}^m |\boldsymbol{a}_i^\top(\boldsymbol{z} - \boldsymbol{z}_0)|^2} \\ &\le \sqrt{\eta^2 + \delta_1} \cdot 2\delta_0, \end{aligned} \tag{14}$$

where in the last inequality we used the fact that with high probability:

$$\frac{1}{m}\sum_{i=1}^{m}|\boldsymbol{a}_i^\top \tilde{\boldsymbol{z}}|^2 \le 1.01, \qquad \forall\, \tilde{\boldsymbol{z}} \in \mathbb{S}^{n-1}.$$

Furthermore,

$$|\mathbb{E}g(\boldsymbol{a}_1^\top \boldsymbol{z}, \boldsymbol{a}_i^\top \boldsymbol{x}) - \mathbb{E}g(\boldsymbol{a}_1^\top \boldsymbol{z}_0, \boldsymbol{a}_i^\top \boldsymbol{x})| \le \mathbb{E}\left[K(\boldsymbol{a}_1)|\boldsymbol{a}_1^\top(\boldsymbol{z}-\boldsymbol{z}_0)|\right] \le \eta\delta_0. \tag{15}$$

Choose $\delta_0 = \frac{\sqrt{2}\varepsilon}{12\eta}$ and $\delta_1 = \min\left(\eta^2, \eta\right)$. Taking the union bound together with (13), (14) and (15), we obtain that with probability at least $1 - 2\exp\left(-c'(\varepsilon,\tau,\eta)m\right)$ it holds

$$\begin{aligned}
&\left|\frac{1}{m}\sum_{i=1}^{m} g(\boldsymbol{a}_i^\top \boldsymbol{z}, \boldsymbol{a}_i^\top \boldsymbol{x}) - \mathbb{E}[g(\boldsymbol{a}_1^\top \boldsymbol{z}, \boldsymbol{a}_1^\top \boldsymbol{x})]\right| \\
&\le \left|\frac{1}{m}\sum_{i=1}^{m} g(\boldsymbol{a}_i^\top \boldsymbol{z}, \boldsymbol{a}_i^\top \boldsymbol{x}) - \frac{1}{m}\sum_{i=1}^{m} g(\boldsymbol{a}_i^\top \boldsymbol{z}_0, \boldsymbol{a}_i^\top \boldsymbol{x})\right| + \left|\frac{1}{m}\sum_{i=1}^{m} g(\boldsymbol{a}_i^\top \boldsymbol{z}_0, \boldsymbol{a}_i^\top \boldsymbol{x}) - \mathbb{E}[g(\boldsymbol{a}_1^\top \boldsymbol{z}_0, \boldsymbol{a}_1^\top \boldsymbol{x})]\right| \\
&\quad + \left|\mathbb{E}[g(\boldsymbol{a}_1^\top \boldsymbol{z}, \boldsymbol{a}_i^\top \boldsymbol{x})] - \mathbb{E}[g(\boldsymbol{a}_1^\top \boldsymbol{z}_0, \boldsymbol{a}_1^\top \boldsymbol{x})]\right| \\
&\le 2\delta_0\sqrt{\eta^2+\delta_1} + \frac{\varepsilon}{3} + \eta\delta_0 \\
&\le \varepsilon
\end{aligned}$$

for all $\boldsymbol{z} \in \Omega$, provided $m \ge C\max\left(\tau^2/\varepsilon^2, 1/\eta^2, 1\right)\cdot\log(\eta/\varepsilon)\cdot n$. Here, the constant $c'(\varepsilon,\tau,\eta) := c\cdot\min\left(\varepsilon^2/\tau^2, \eta^2, 1\right)$ for some universal constant $c > 0$. ■

5.4. Proof of Lemma 3.1

Proof. Note that $\nabla F(\boldsymbol{z}) = \frac{1}{m}\sum_{i=1}^{m}\nabla f_i(\boldsymbol{z})$ and $\langle\nabla f_i(\boldsymbol{z}), \boldsymbol{z}\rangle = \Psi_u(\boldsymbol{a}_i^\top \boldsymbol{z}, \boldsymbol{a}_i^\top \boldsymbol{x})(\boldsymbol{a}_i^\top \boldsymbol{z})$. From Lemma (6.2) we have

$$\Psi_u(\boldsymbol{a}_i^\top \boldsymbol{z}, \boldsymbol{a}_i^\top \boldsymbol{x})(\boldsymbol{a}_i^\top \boldsymbol{z}) \ge (\boldsymbol{a}_i^\top \boldsymbol{z})^2 - |(\boldsymbol{a}_i^\top \boldsymbol{z})(\boldsymbol{a}_i^\top \boldsymbol{x})|.$$

Set $U_i = \boldsymbol{a}_i^\top \boldsymbol{z}/\|\boldsymbol{z}\|, V_i = \boldsymbol{a}_i^\top \boldsymbol{x}$. Then from Lemma 6.6 we have

$$\mathbb{E}[|U_iV_i|] = \frac{2}{\pi}\left(\tau + \sigma\arctan\frac{\sigma}{\tau}\right).$$

It then follows that

$$\frac{1}{\|\boldsymbol{z}\|^2}\mathbb{E}[\langle\nabla f_i(\boldsymbol{z}), \boldsymbol{z}\rangle] \ge 1 - \frac{1}{\|\boldsymbol{z}\|}\cdot\mathbb{E}[|U_iV_i|] \ge 1 - \frac{1}{\|\boldsymbol{z}\|}\cdot\frac{2}{\pi}\left(\tau + \sigma\arctan\frac{\sigma}{\tau}\right).$$

From Lemma (6.2), it is easy to check $\frac{1}{\|\boldsymbol{z}\|^2}\langle\nabla f_i(\boldsymbol{z}), \boldsymbol{z}\rangle$ is continuous satisfying the conditions in Lemma 2.1 with $\tau = O(1)$ and $\eta = O(1/\beta)$. Thus for any $\delta_0 > 0$ there exists $\varepsilon_0 > 0$ such that with probability at least $1 - 2\exp(-c\delta_0^2 m)$ for $m \ge C\delta_0^{-2}\log(1/\beta)n$ we have

$$\frac{1}{\|\boldsymbol{z}\|^2}\langle\nabla F(\boldsymbol{z}), \boldsymbol{z}\rangle = \frac{1}{m}\sum_{i=1}^{m}\frac{1}{\|\boldsymbol{z}\|^2}\langle\nabla f_i(\boldsymbol{z}), \boldsymbol{z}\rangle \ge \varepsilon_0$$

for all $\|\boldsymbol{z}\| \ge \frac{2}{\pi}\left(\tau + \sigma\arctan\frac{\sigma}{\tau}\right) + \delta_0$ (This region is a compact set with respect to $\lambda = \beta/\|\boldsymbol{z}\|$). Here, C and c are some universal positive constants. The lemma is proved. ■

5.5. Proof of Lemma 3.2

Proof. Recall that $\langle \nabla F(\boldsymbol{z}), \boldsymbol{x}\rangle = \frac{1}{m}\sum_{i=1}^m \Psi_u(\boldsymbol{a}_i^\top \boldsymbol{z}, \boldsymbol{a}_i^\top \boldsymbol{x})(\boldsymbol{a}_i^\top \boldsymbol{x})$. Let $\boldsymbol{a} \sim \mathcal{N}(0, I_n)$ be standard Gaussian. Then $\mathbb{E}[\langle \nabla F(\boldsymbol{z}), \boldsymbol{x}\rangle] = \mathbb{E}[\Psi_u(\boldsymbol{a}^\top \boldsymbol{z}, \boldsymbol{a}^\top \boldsymbol{x})(\boldsymbol{a}^\top \boldsymbol{x})]$. Set

$$g(\boldsymbol{z}) = \frac{1}{\|\boldsymbol{z}\|}\mathbb{E}[\langle \nabla F(\boldsymbol{z}), \boldsymbol{x}\rangle] = \frac{1}{\|\boldsymbol{z}\|}\mathbb{E}[\Psi_u(\boldsymbol{a}^\top \boldsymbol{z}, \boldsymbol{a}^\top \boldsymbol{x})(\boldsymbol{a}^\top \boldsymbol{x})].$$

Using the notation U, V, W and $\lambda = \beta/\|\boldsymbol{z}\|$ defined in (A3) and expanding out Ψ_u via (10), it yields

$$g(\boldsymbol{z}) = \sigma - \frac{\lambda}{\beta}\mathbb{E}[\operatorname{sgn}(UV)V^2 \mathbb{1}_{A^c}] + \frac{1}{2\lambda^2}\,\mathbb{E}[U^3V^{-1})\mathbb{1}_A] - \Big(\frac{1}{2} + \frac{1}{\beta}\Big)\mathbb{E}[UV\mathbb{1}_A]$$

where $A := \{|U| \le \lambda |V|\}$. Note that $g(\boldsymbol{z})$ now depends on λ and σ as $\boldsymbol{z}$ is completely determined by λ and σ once β is fixed. Set $B(\lambda, \sigma) := \frac{2}{\pi\tau}(\mu_-^{-4} - \mu_+^{-4})$. By Corollary 6.5 we have

$$\begin{aligned}\frac{\partial g}{\partial \lambda} &= -\frac{1}{\beta}\mathbb{E}[\operatorname{sgn}(UV)V^2\mathbb{1}_{A^c}] + \frac{\lambda}{\beta}\cdot B(\lambda,\sigma) - \frac{1}{\lambda^3}\,\mathbb{E}[U^3V^{-1})\mathbb{1}_A] \\ &\quad + \frac{1}{2\lambda^2}\cdot \lambda^3 B(\lambda,\sigma) - \Big(\frac{1}{2}+\frac{1}{\beta}\Big)\lambda B(\lambda,\sigma) \\ &= -\frac{1}{\beta}\mathbb{E}[\operatorname{sgn}(UV)V^2\mathbb{1}_{A^c}] - \frac{1}{\lambda^3}\,\mathbb{E}[U^3V^{-1})\mathbb{1}_A].\end{aligned}$$

Also by Corollary 6.5, we know

$$\mathbb{E}[U^3V^{-1})\mathbb{1}_A] = \frac{2}{\pi\tau}\int_0^{\lambda} t^3\left(\mu_-^{-4} + \mu_+^{-4}\right)\, dt \ge 0.$$

Furthermore, note that $A^c = \{|U| \ge \lambda|V|\} = \{|V| < \lambda^{-1}|U|\}$. By switching the role of U and V we have

$$\mathbb{E}[\operatorname{sgn}(UV)V^2\mathbb{1}_{A^c}] = \mathbb{E}[\operatorname{sgn}(UV)U^2\mathbb{1}_{A'}] = \frac{2}{\pi\tau}\int_0^{\lambda^{-1}} t^2\left(\mu_-^{-4} - \mu_+^{-4}\right)\, dt \ge 0$$

where $A' := \{|U| \le \lambda^{-1}|V|\}$. Therefore g is a decreasing function in λ, which means that g is increasing with respect to $\|\boldsymbol{z}\|$.

We would like to prove that $g(\boldsymbol{z}) < 0$ for $\varepsilon_0 \le \|\boldsymbol{z}\| \le 1$ and $\sigma_0 \le \sigma \le 1 - \sigma_0$. To do so we only need to show $g(\boldsymbol{z}) < 0$ for $\|\boldsymbol{z}\| = 1$, i.e. $\lambda = \beta$ and $\sigma_0 \le \sigma \le 1 - \sigma_0$. Now, note that

$$\begin{aligned}\mathbb{E}[\operatorname{sgn}(UV)V^2\mathbb{1}_{A^c}] &= \mathbb{E}[\operatorname{sgn}(UV)V^2] - \mathbb{E}[\operatorname{sgn}(UV)V^2\mathbb{1}_A] \\ &= \frac{2}{\pi}\Big(\tau\sigma + \arctan\frac{\sigma}{\tau}\Big) - \mathbb{E}[\operatorname{sgn}(UV)V^2\mathbb{1}_A].\end{aligned}$$

Thus for $\lambda = \beta$, again applying Corollary 6.5 we obtain

$$g(\boldsymbol{z}) = \sigma - \frac{2}{\pi}\Big(\tau\sigma + \arctan\frac{\sigma}{\tau}\Big) + \int_0^{\beta}\left(1 + \frac{t^3}{2\beta^2} - \Big(\frac{1}{2}+\frac{1}{\beta}\Big)t\right) B(t,\sigma)\, dt. \tag{16}$$

To establish $g(\boldsymbol{z}) < 0$ here, we observe that

$$\frac{\partial g(\boldsymbol{z})}{\partial \beta} = \int_0^{\beta} \left(\frac{1}{\beta}\Big(\frac{t}{\beta}\Big) - \Big(\frac{t}{\beta}\Big)^3 \right) B(t,\sigma)\, dt > 0.$$

Thus $g(\boldsymbol{z})$ is increasing with respect to β. Hence, it suffices to show that $g(\boldsymbol{z}) < 0$ for $\beta = 1/2$. Expanding $B(t,\sigma)$ yields

$$B(t,\sigma) = \frac{16\tau^3 \sigma t(1+t^2)}{\pi\left((1+t^2)^2 - 4\sigma^2 t^2\right)^2} =: \tau^3 \sigma\, Q(t,\sigma),$$

where $Q(t,\sigma) := \frac{16t(1+t^2)}{\pi((1+t^2)^2-4\sigma^2t^2)^2}$. It follows that for $\beta = 1/2$ we have

$$\frac{1}{\sigma\tau^3} g(\boldsymbol{z}) = \frac{1}{\tau^3}\left(1 - \frac{2}{\pi}\Big(\tau + \frac{1}{\sigma}\arctan\frac{\sigma}{\tau}\Big)\right) + \int_0^{1/2} \left(1 + 2t^3 - 2.5t\right) Q(t,\sigma)\, dt. \tag{17}$$

Clearly $Q(t,\sigma) \le Q(t,1)$. Next, integrating rational functions by partial fractions, we can obtain

$$\begin{aligned}\int_0^{1/2} \left(1+2t^3-2.5t\right) Q(t,1)\ dt &= \frac{8}{\pi}\int_0^{1/2} \frac{(4t^3-5t+2)(t^2+1)t}{(t^2-1)^4}\ dt \\ &= \frac{4}{\pi}\left(\frac{35}{27} - \ln 3\right) < 0.26.\end{aligned}$$

Meanwhile, the term before the integral in (17) is a function of σ and it is decreasing. Indeed, by Corollary 6.5 where we set $\lambda = \infty$, we have

$$\begin{aligned} P(\sigma) &:= \frac{1}{\tau^3}\left(1 - \frac{2}{\pi}\Big(\tau + \frac{1}{\sigma}\arctan\frac{\sigma}{\tau}\Big)\right) \\ &= \frac{1}{\tau^3\sigma}\mathbb{E}\left[UV - \operatorname{sgn}(UV)V^2\right] \\ &= \frac{1}{\tau^3\sigma}\int_0^{\infty} (t-1)B(t,\sigma)\ dt \\ &= \frac{16}{\pi}\int_0^{\infty} \frac{(t-1)(1+t^2)t}{\left[(1+t^2)^2 - 4t^2\sigma^2\right]^2}\ dt. \end{aligned}$$

Making a substitution $t = \frac{1}{u}$, we obtain

$$\int_1^{\infty} \frac{(t-1)(1+t^2)t}{\left[(1+t^2)^2-4t^2\sigma^2\right]^2}\ dt = -\int_0^{1} \frac{(u-1)(1+u^2)u^2}{\left[(1+u^2)^2-4u^2\sigma^2\right]^2}\ du.$$

It gives

$$P(\sigma) = -\frac{16}{\pi}\int_0^{1} \frac{(1-t)^2(1+t^2)t}{\left[(1+t^2)^2-4t^2\sigma^2\right]^2}\ dt,$$

which is decreasing with respect to σ. Thus the maximum of $P(\sigma)$ is achieved at $\sigma = 0$ and we have

$$
\begin{aligned}
\frac{1}{\tau^3}\left(1-\frac{2}{\pi}\Big(\tau+\frac{1}{\sigma}\arctan\frac{\sigma}{\tau}\Big)\right) &\le \lim_{\sigma\to 0}\left(1-\frac{2}{\pi}\Big(1+\frac{\arctan\sigma}{\sigma}\Big)\right)\\
&= 1-\frac{4}{\pi}\le -0.27.
\end{aligned}
$$

Thus we have shown by combining the two estimates that $\frac{1}{\sigma\tau^3}g(\boldsymbol{z}) < -0.01$. So $g(\boldsymbol{z}) < -\delta_0$ for some $\delta_0 > 0$.

From Lemma (6.2), one can easily check that $\frac{1}{\|\boldsymbol{z}\|}\langle \nabla f_i(\boldsymbol{z}), \boldsymbol{x}\rangle$ is continuous satisfying the conditions in Lemma 2.1 with $\tau = O(1)$ and $\eta = O(1/\beta)$. Hence, the lemma follows by applying Lemma 2.1 directly. ■

5.6. *Proof of Lemma 3.3*

Proof. Again we start from $\langle \nabla F(\boldsymbol{z}), \boldsymbol{x}\rangle = \frac{1}{m}\sum_{i=1}^m \Psi_u(\boldsymbol{a}_i^\top \boldsymbol{z}, \boldsymbol{a}_i^\top \boldsymbol{x})(\boldsymbol{a}_i^\top \boldsymbol{x})$. Let $\boldsymbol{a} \sim \mathcal{N}(0, I_n)$ be standard Gaussian. Then $\mathbb{E}[\langle \nabla F(\boldsymbol{z}), \boldsymbol{x}\rangle] = \mathbb{E}[\Psi_u(\boldsymbol{a}^\top \boldsymbol{z}, \boldsymbol{a}^\top \boldsymbol{x})(\boldsymbol{a}^\top \boldsymbol{x})]$. First we consider $\sigma = 1$, for which $\boldsymbol{z} = \|\boldsymbol{z}\|\boldsymbol{x}$ and $\boldsymbol{a}^\top \boldsymbol{z} = \|\boldsymbol{z}\|\boldsymbol{a}^\top \boldsymbol{x}$. Set $\lambda = \beta/\|\boldsymbol{z}\|$ as usual. One can easily check via (10) that

$$
\Psi_u(\boldsymbol{a}^\top \boldsymbol{z}, \boldsymbol{a}^\top \boldsymbol{x})(\boldsymbol{a}^\top \boldsymbol{x}) = \begin{cases} (\|\boldsymbol{z}\|-1)(\boldsymbol{a}^\top \boldsymbol{x})^2, & \|\boldsymbol{z}\| > \beta;\\ \frac{\|\boldsymbol{z}\|^3}{2\beta^2}(\boldsymbol{a}^\top \boldsymbol{x})^2 + (\frac{1}{2}-\frac{1}{\beta})\|\boldsymbol{z}\|(\boldsymbol{a}^\top \boldsymbol{x})^2, & \|\boldsymbol{z}\| \le \beta. \end{cases}
$$

Thus $\Psi_u(\boldsymbol{a}^\top \boldsymbol{z}, \boldsymbol{a}^\top \boldsymbol{x})(\boldsymbol{a}^\top \boldsymbol{x}) \le -\delta_0(\boldsymbol{a}^\top \boldsymbol{x})^2$ for some $\delta_0 > 0$. It follows that $\mathbb{E}[\langle \nabla F(\boldsymbol{z}), \boldsymbol{x}\rangle] = \mathbb{E}[\Psi_u(\boldsymbol{a}^\top \boldsymbol{z}, \boldsymbol{a}^\top \boldsymbol{x})(\boldsymbol{a}^\top \boldsymbol{x})] \le -\delta_0$. Now by continuity $\mathbb{E}[\langle \nabla F(\boldsymbol{z}), \boldsymbol{x}\rangle] \le -\delta_1$ for some $\sigma_0, \delta_1 > 0$ for all $\varepsilon_0 \le \|\boldsymbol{z}\| \le 1-\varepsilon_0$ and $\sigma \ge 1-\sigma_0$.

To show that $\langle \nabla F(\boldsymbol{z}), \boldsymbol{x}\rangle < -\epsilon$ with high probability for $m \ge Cn$ for all $\varepsilon_0 \le \|\boldsymbol{z}\| \le 1-\varepsilon_0$ and $\sigma \ge 1-\sigma_0$. Observe that $\Psi_u(\boldsymbol{a}^\top \boldsymbol{z}, \boldsymbol{a}^\top \boldsymbol{x})(\boldsymbol{a}^\top \boldsymbol{x})$ is a Lipschitz continuous function of $\boldsymbol{z}$ on this region. The conditions of Lemma 2.1 are met by applying Lemma (6.2). The lemma now follows. ■

5.7. *Proof of Lemma 3.4*

Proof. First we assume $\sigma = 0$, and prove $\mathbb{E}[D_{\boldsymbol{x}}^2 F(\boldsymbol{z})] < -5\varepsilon_0$ if $\|\boldsymbol{z}\| \le 1+\delta_0$ for some $\varepsilon_0, \delta_0 > 0$. Let $\boldsymbol{a} \sim \mathcal{N}(0, I_n)$ be standard Gaussian. Set

$$
G(\boldsymbol{z}) := (\boldsymbol{a}^\top \boldsymbol{x})^2 + \frac{3}{2\beta^2}(\boldsymbol{a}^\top \boldsymbol{z})^2 \mathbb{1}_R - \Big(\frac{1}{2}+\frac{1}{\beta}\Big)(\boldsymbol{a}^\top \boldsymbol{x})^2 \mathbb{1}_R
$$

where $R := \{|\boldsymbol{a}^\top \boldsymbol{z}| < \beta|\boldsymbol{a}^\top \boldsymbol{x}|\}$. From (12) with $\boldsymbol{v} = \boldsymbol{x}$ we have $D_{\boldsymbol{x}}^2 f_i(\boldsymbol{z}) \le G(\boldsymbol{z})$. As before let $\lambda = \beta/\|\boldsymbol{z}\|$, $U = \boldsymbol{a}^\top \boldsymbol{z}/\|\boldsymbol{z}\|$ and $V = \boldsymbol{a}^\top \boldsymbol{x}$. We have

$$
\mathbb{E}[G(\boldsymbol{z})] = 1 + \frac{3}{2\lambda^2}\mathbb{E}[U^2 \mathbb{1}_A] - \Big(\frac{1}{2}+\frac{1}{\beta}\Big)\mathbb{E}[V^2 \mathbb{1}_A] =: g(\lambda)
$$

where $A = \{|U| \le \lambda|V|\}$. Observe that by Corollary 6.4,

$$
g'(\lambda) = -\frac{3}{\lambda^3}\mathbb{E}[U^2 \mathbb{1}_A] + \frac{3}{\pi\tau}(\mu_+^{-4}+\mu_-^{-4}) - \Big(\frac{1}{2}+\frac{1}{\beta}\Big)\frac{2}{\pi\tau}(\mu_+^{-4}+\mu_-^{-4}) < 0.
$$

So $g(\lambda)$ is decreasing with respect to λ, which also means $\mathbb{E}[G(\boldsymbol{z})]$ is increasing with respect to $\|\boldsymbol{z}\|$. We show that $\mathbb{E}[G(\boldsymbol{z})] < -5\varepsilon_0$ for $\|\boldsymbol{z}\| \le 1$, and it suffices to show this for $\|\boldsymbol{z}\| = 1$, i.e. $g(\lambda) < -5\varepsilon_0$.

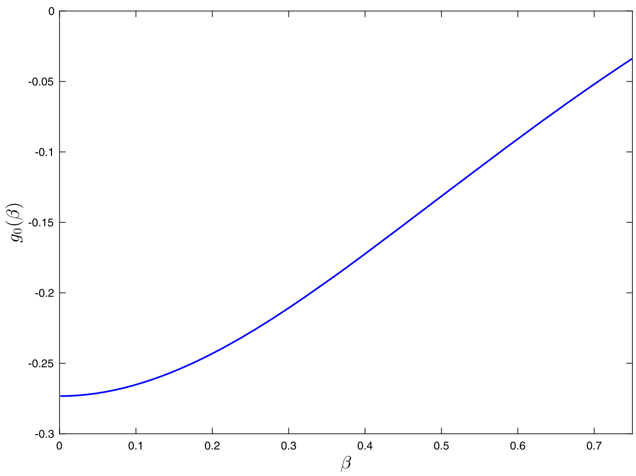

Fig. 6. $g_0(\beta)$.

Since $\sigma = 0$ (and hence $\tau = 1$) we have simple closed form solution for $g(\lambda)$, which by Corollary 6.4 is

$$g(\lambda) = 1 + \frac{3}{2\lambda^2} \cdot \frac{4}{\pi} \int_0^\lambda \frac{t^2}{(1+t^2)^2}\, dt - \left(\frac{1}{2} + \frac{1}{\beta}\right) \cdot \frac{4}{\pi} \int_0^\lambda \frac{1}{(1+t^2)^2}\, dt$$
$$= 1 + \frac{3}{\pi\lambda^2}\left(\arctan\lambda - \frac{\lambda}{1+\lambda^2}\right) - \frac{\beta+2}{\pi\beta}\left(\arctan\lambda + \frac{\lambda}{1+\lambda^2}\right).$$

Since $\|\boldsymbol{z}\| = 1$, it follows that

$$g(\lambda) = 1 - \frac{3+\beta^2+2\beta}{\pi(1+\beta^2)\beta} + \frac{3-\beta^2-2\beta}{\pi\beta^2} \cdot \arctan\beta \quad := g_0(\beta).$$

The graph of this function $g_0(\beta)$ is shown in Fig. 6; we check that $g_0(\beta) < -0.03$ for all $\beta \in (0, \frac{3}{4}]$. Taking $\varepsilon_0 = 0.006$ we obtain the desired result. Since $g(\lambda)$ is continuous, for a sufficiently small $\delta_0 > 0$ we have $g(\lambda) < -4\varepsilon_0$ for all $\|\boldsymbol{z}\| \le 1 + \delta_0$.

To prove the lemma for the region $\|\boldsymbol{z}\| \le 1 + \delta_0$ and $\sigma \le \sigma_0$, we need to use Lipschitz condition and Lemma 2.1. Our challenge is that the function $G(\boldsymbol{z})$ is discontinuous with a jump discontinuity when $|\boldsymbol{a}^\top \boldsymbol{z}| = \beta|\boldsymbol{a}^\top \boldsymbol{x}|$. To get around this problem we smooth out the function by introducing

$$H_p(u,v) := v^2 + \frac{3}{2\beta^2}u^2 \mathbb{1}_S - \left(\frac{1}{2} + \frac{1}{\beta}\right)v^2 \mathbb{1}_S + \left(\frac{1}{\beta} - 1\right)\frac{|u|^p}{\beta^p |v|^{p-2}}\mathbb{1}_S$$

where $p > 0$ and $S = \{(u,v) : \ |u| < \beta|v|\}$. A key observation is $H_p(u,v)$ is continuous and satisfies the Lipschitz condition with respect to u in Lemma 2.1 (here we need the property $|u| < \beta|v|$ on S). Clearly $H_p(\boldsymbol{a}^\top \boldsymbol{z}, \boldsymbol{a}^\top \boldsymbol{x}) \ge G(\boldsymbol{z})$. Note that

$$\frac{|u|^p}{\beta^p |v|^{p-2}}\mathbb{1}_S = \left(\frac{|u|}{\beta|v|}\right)^p |v|^2 \mathbb{1}_S \to 0 \quad \text{as} \quad p \to \infty.$$

It means that $\mathbb{E}[H_p(\boldsymbol{a}^\top \boldsymbol{z}, \boldsymbol{a}^\top \boldsymbol{x})] \longrightarrow \mathbb{E}[G(\boldsymbol{z})]$ as $p \to \infty$. Hence for $0 \le \|\boldsymbol{z}\| \le 1 + \delta_0$, by taking $p = p_0$ sufficiently large we obtain $\mathbb{E}[H_{p_0}(\boldsymbol{a}^\top \boldsymbol{z}, \boldsymbol{a}^\top \boldsymbol{x})] < -3\varepsilon_0$. Because $\mathbb{E}[H_{p_0}(\boldsymbol{a}^\top \boldsymbol{z}, \boldsymbol{a}^\top \boldsymbol{x})]$ is a continuous function of σ, there exists a $\sigma_0 > 0$ such that $\mathbb{E}[H_{p_0}(\boldsymbol{a}^\top \boldsymbol{z}, \boldsymbol{a}^\top \boldsymbol{x})] < -2\varepsilon_0$ for $0 < \|\boldsymbol{z}\| \le 1 + \delta_0$ and $\sigma \le \sigma_0$. Finally,

$$D_{\boldsymbol{x}}^2 F(\boldsymbol{z}) \leq \frac{1}{m}\sum_{i=1}^m H_{p_0}(\boldsymbol{a}_i^\top \boldsymbol{z}, \boldsymbol{a}_i^\top \boldsymbol{x}).$$

Note that $H_{p_0}(\boldsymbol{a}_i^\top \boldsymbol{z}, \boldsymbol{a}_i^\top \boldsymbol{x})$ are subexponential random variables with subexponential norm $\tau = O(1/\beta)$. On the other hand, $H_{p_0}(\boldsymbol{a}_i^\top \boldsymbol{z}, \boldsymbol{a}_i^\top \boldsymbol{x})$ is continuous satisfying the Lipschitz type condition in Lemma 2.1 with $\eta = O(1/\beta)$. It then follows from Lemma 2.1 that with probability at least $1 - 2\exp(-c\beta^2 m)$ for $m \geq C \cdot 1/\beta^2 \log(1/\beta)n$, it holds $D_{\boldsymbol{x}}^2 F(\boldsymbol{z}) \leq -\varepsilon_0$ for all $\boldsymbol{z}$ with $0 \leq \|\boldsymbol{z}\| \leq 1 + \delta_0$ and $\sigma \leq \sigma_0$.

To prove the lemma for $\boldsymbol{z} \in B_{\delta_0}(0)$ we use virtually identical technique. It is easily seen $\mathbb{E}[H_p(0)] = \mathbb{E}[G(0)] = \frac{1}{2} - \frac{1}{\beta} < 0$. By continuity $\mathbb{E}[H_p(\boldsymbol{z})] < -\varepsilon_1$ for $\boldsymbol{z} \in B_{\delta_0}(0)$ for some $\delta_0, \varepsilon_1 > 0$. Now using Lemma 6.1 and Lemma 2.1 the same argument as in the previous region applies to prove this case of the lemma. ∎

5.8. *Proof of Lemma 3.5*

Proof. Let $\boldsymbol{a} \sim \mathcal{N}(0, I_n)$ be standard Gaussian. We follow the same strategy of evaluating an expectation and prove the lemma using Lipschitz condition and Lemma 2.1. To begin with, we introduce an auxiliary function

$$G(\boldsymbol{a}^\top \boldsymbol{z}, \boldsymbol{a}^\top \boldsymbol{x}, \boldsymbol{a}^\top \boldsymbol{v}) := (\boldsymbol{a}^\top \boldsymbol{v})^2 + \left[\frac{3}{2\beta^2}\frac{|\boldsymbol{a}^\top \boldsymbol{z}|^2}{|\boldsymbol{a}^\top \boldsymbol{x}|^2} \cdot |\boldsymbol{a}^\top \boldsymbol{v}|^2 - (\frac{1}{2} + \frac{1}{\beta})(\boldsymbol{a}^\top \boldsymbol{v})^2\right] \chi_1\left(\frac{|\boldsymbol{a}^\top \boldsymbol{z}|}{|\boldsymbol{a}^\top \boldsymbol{x}|}\right) \chi_2\left(\frac{|\boldsymbol{a}^\top \boldsymbol{v}|}{M_0 |\boldsymbol{a}^\top \boldsymbol{x}|}\right),$$

where

$$\chi_1(x) := \begin{cases} 1 & \text{if} \quad 0 \leq x \leq \beta, \\ 1 + \frac{\beta}{\delta_0} - \frac{1}{\delta_0} x & \text{if} \quad \beta \leq x \leq \beta + \delta_0, \\ 0 & \text{if} \quad x > \beta + \delta_0, \end{cases}$$

with $\delta_0 = \sqrt{\frac{2\beta + \beta^2}{3}} - \beta$, and $\chi_2(x) \in C_c^\infty(\mathbb{R})$ is a function satisfying $0 \leq \chi_2(x) \leq 1$ for all x, $\chi_2(x) = 1$ for $|x| \leq 1$ and $\chi_2(x) = 0$ for $|x| \geq 2$. Here, M_0 is a positive constant which will be made sufficiently large. It is easy to check that $G(\boldsymbol{a}^\top \boldsymbol{z}, \boldsymbol{a}^\top \boldsymbol{x}, \boldsymbol{a}^\top \boldsymbol{v})$ is continuous with respect to $\boldsymbol{z}$ and $\boldsymbol{v}$. Furthermore, for some sufficiently large M_0, it follows from (12) that $D_{\boldsymbol{v}}^2 f_i(\boldsymbol{z}) \geq G(\boldsymbol{a}_i^\top \boldsymbol{z}, \boldsymbol{a}_i^\top \boldsymbol{x}, \boldsymbol{a}_i^\top \boldsymbol{v})$. It immediately gives

$$D_{\boldsymbol{v}}^2 F(\boldsymbol{z}) \geq \frac{1}{m}\sum_{i=1}^m G(\boldsymbol{a}_i^\top \boldsymbol{z}, \boldsymbol{a}_i^\top \boldsymbol{x}, \boldsymbol{a}_i^\top \boldsymbol{v}). \tag{18}$$

Thus, to prove the lemma we only need to estimate $\frac{1}{m}\sum_{i=1}^m G(\boldsymbol{a}_i^\top \boldsymbol{z}, \boldsymbol{a}_i^\top \boldsymbol{x}, \boldsymbol{a}_i^\top \boldsymbol{v})$. We claim that $G(\boldsymbol{a}^\top \boldsymbol{z}, \boldsymbol{a}^\top \boldsymbol{x}, \boldsymbol{a}^\top \boldsymbol{v})$ satisfies the Lipschitz type condition with respect to $\boldsymbol{z}, \boldsymbol{v}$ in Lemma 2.1 with subgaussian norms $\eta = O(1/\beta^{2.5})$ and $\eta = O(1/\beta)$, respectively. Note that $G(\boldsymbol{a}^\top \boldsymbol{z}, \boldsymbol{a}^\top \boldsymbol{x}, \boldsymbol{a}^\top \boldsymbol{v})$ is a subexponential with subexponential norm $\tau = O(1/\beta)$. It then follows from Lemma 2.1 that with probability at least $1 - 2\exp(-c\epsilon^2\beta^2 m)$ we have

$$\frac{1}{m}\sum_{i=1}^m G(\boldsymbol{a}_i^\top \boldsymbol{z}, \boldsymbol{a}_i^\top \boldsymbol{x}, \boldsymbol{a}_i^\top \boldsymbol{v}) \geq \mathbb{E}[G(\boldsymbol{a}^\top \boldsymbol{z}, \boldsymbol{a}^\top \boldsymbol{x}, \boldsymbol{a}^\top \boldsymbol{v})] - \epsilon \tag{19}$$

for all $\boldsymbol{z} \in B_{\delta_0}(\boldsymbol{x})$ and unit vectors $\boldsymbol{v}$, provided $m \geq C\epsilon^{-2}\beta^{-2}\log(1/\beta)n$. Here, C and c are positive constants.

On the other hand, note that $\chi_1(x)$ is enlarged from the set $R = \{|\boldsymbol{a}^\top \boldsymbol{z}| < \beta|\boldsymbol{a}^\top \boldsymbol{x}|\}$. It then gives

$$G(\boldsymbol{a}^\top \boldsymbol{x}, \boldsymbol{a}^\top \boldsymbol{x}, \boldsymbol{a}^\top \boldsymbol{v}) = (\boldsymbol{a}^\top \boldsymbol{v})^2 + (\frac{3}{2\beta^2} - \frac{1}{2} - \frac{1}{\beta})(\boldsymbol{a}^\top \boldsymbol{v})^2 \cdot \chi_2\left(\frac{|\boldsymbol{a}^\top \boldsymbol{v}|}{M_0|\boldsymbol{a}^\top \boldsymbol{x}|}\right) \geq (\boldsymbol{a}^\top \boldsymbol{v})^2.$$

Hence $\mathbb{E}[G(\boldsymbol{a}^\top \boldsymbol{x}, \boldsymbol{a}^\top \boldsymbol{x}, \boldsymbol{a}^\top \boldsymbol{v})] \geq 1$. Since $G(\boldsymbol{a}^\top \boldsymbol{z}, \boldsymbol{a}^\top \boldsymbol{x}, \boldsymbol{a}^\top \boldsymbol{v})$ is continuous with respect to $\boldsymbol{z}$ and $\boldsymbol{v}$, and $\boldsymbol{v}$ is on the unit sphere which is compact, we know that

$$\mathbb{E}[G(\boldsymbol{a}^\top \boldsymbol{z}, \boldsymbol{a}^\top \boldsymbol{x}, \boldsymbol{a}^\top \boldsymbol{v})] \geq 0.7 \tag{20}$$

for $\boldsymbol{z}$ in a neighborhood $\boldsymbol{z} \in B_{\delta_0}(\boldsymbol{x})$ for all unit vectors $\boldsymbol{v}$.

Combining (18), (19) and (20), we obtain that with probability at least $1 - 2\exp(-c\beta^2 m)$ for $m \geq C\beta^{-2}\log(1/\beta)n$ it holds

$$D_{\boldsymbol{v}}^2 F(\boldsymbol{z}) \geq \frac{1}{m}\sum_{i=1}^m G(\boldsymbol{a}_i^\top \boldsymbol{z}, \boldsymbol{a}_i^\top \boldsymbol{x}, \boldsymbol{a}_i^\top \boldsymbol{v}) \geq 0.5$$

for all $\boldsymbol{z} \in B_{\delta_0}(\boldsymbol{x})$ and unit vectors $\boldsymbol{v}$.

Finally, it remains to prove the claim that $G(\boldsymbol{a}^\top \boldsymbol{z}, \boldsymbol{a}^\top \boldsymbol{x}, \boldsymbol{a}^\top \boldsymbol{v})$ satisfies the Lipschitz type condition with respect to $\boldsymbol{z}, \boldsymbol{v}$ in Lemma 2.1 with subgaussian norms $\eta = O(1/\beta^{2.5})$ and $\eta = O(1/\beta)$, respectively. Indeed, for the second term of $G(\boldsymbol{a}^\top \boldsymbol{z}, \boldsymbol{a}^\top \boldsymbol{x}, \boldsymbol{a}^\top \boldsymbol{v})$. Note that

$$\begin{aligned} L_1(\boldsymbol{a}^\top \boldsymbol{z}, \boldsymbol{a}^\top \boldsymbol{x}, \boldsymbol{a}^\top \boldsymbol{v}) &:= \frac{|\boldsymbol{a}^\top \boldsymbol{z}|^2}{|\boldsymbol{a}^\top \boldsymbol{x}|^2} \cdot |\boldsymbol{a}^\top \boldsymbol{v}|^2 \chi_1\left(\frac{|\boldsymbol{a}^\top \boldsymbol{z}|}{|\boldsymbol{a}^\top \boldsymbol{x}|}\right) \chi_2\left(\frac{|\boldsymbol{a}^\top \boldsymbol{v}|}{M_0|\boldsymbol{a}^\top \boldsymbol{x}|}\right) \\ &= \frac{|\boldsymbol{a}^\top \boldsymbol{z}|^2}{|\boldsymbol{a}^\top \boldsymbol{x}|^2} \chi_1\left(\frac{|\boldsymbol{a}^\top \boldsymbol{z}|}{|\boldsymbol{a}^\top \boldsymbol{x}|}\right) \cdot \frac{|\boldsymbol{a}^\top \boldsymbol{v}|^2}{|\boldsymbol{a}^\top \boldsymbol{x}|^2} \chi_2\left(\frac{|\boldsymbol{a}^\top \boldsymbol{v}|}{M_0|\boldsymbol{a}^\top \boldsymbol{x}|}\right) \cdot |\boldsymbol{a}^\top \boldsymbol{x}|^2 \\ &=: \psi_1\left(\frac{|\boldsymbol{a}^\top \boldsymbol{z}|}{|\boldsymbol{a}^\top \boldsymbol{x}|}\right) \psi_2\left(\frac{|\boldsymbol{a}^\top \boldsymbol{v}|}{|\boldsymbol{a}^\top \boldsymbol{x}|}\right) |\boldsymbol{a}^\top \boldsymbol{x}|^2. \end{aligned}$$

Note that $\psi_1(t)$ is a Lipschitz function with Lipschitz norm $O(1/\delta_0)$ and $\psi_2(t)$ is a bound function with $|\psi_2(t)| \leq 4M_0^2$. Here we use the condition $\beta < 1$. It gives that

$$\left|L_1(\boldsymbol{a}^\top \boldsymbol{z}_1, \boldsymbol{a}^\top \boldsymbol{x}, \boldsymbol{a}^\top \boldsymbol{v}) - L_1(\boldsymbol{a}^\top \boldsymbol{z}_2, \boldsymbol{a}^\top \boldsymbol{x}, \boldsymbol{a}^\top \boldsymbol{v})\right| \lesssim \frac{M_0^2}{\delta_0} \cdot |\boldsymbol{a}^\top(\boldsymbol{z}_1 - \boldsymbol{z}_2)||\boldsymbol{a}^\top \boldsymbol{x}|. \tag{21}$$

Similarly, for the third term of $G(\boldsymbol{a}^\top \boldsymbol{z}, \boldsymbol{a}^\top \boldsymbol{x}, \boldsymbol{a}^\top \boldsymbol{v})$, we know

$$L_2 := (\boldsymbol{a}^\top \boldsymbol{v})^2 \chi_1\left(\frac{|\boldsymbol{a}^\top \boldsymbol{z}|}{|\boldsymbol{a}^\top \boldsymbol{x}|}\right) \chi_2\left(\frac{|\boldsymbol{a}^\top \boldsymbol{v}|}{M_0|\boldsymbol{a}^\top \boldsymbol{x}|}\right) = \chi_1\left(\frac{|\boldsymbol{a}^\top \boldsymbol{z}|}{|\boldsymbol{a}^\top \boldsymbol{x}|}\right) \psi_2\left(\frac{|\boldsymbol{a}^\top \boldsymbol{v}|}{|\boldsymbol{a}^\top \boldsymbol{x}|}\right) |\boldsymbol{a}^\top \boldsymbol{x}|^2.$$

Due to the Lipschitz property of $\chi_1(t)$, we also have

$$\left|L_2(\boldsymbol{a}^\top \boldsymbol{z}_1, \boldsymbol{a}^\top \boldsymbol{x}, \boldsymbol{a}^\top \boldsymbol{v}) - L_2(\boldsymbol{a}^\top \boldsymbol{z}_2, \boldsymbol{a}^\top \boldsymbol{x}, \boldsymbol{a}^\top \boldsymbol{v})\right| \lesssim \frac{M_0^2}{\delta_0} \cdot |\boldsymbol{a}^\top(\boldsymbol{z}_1 - \boldsymbol{z}_2)||\boldsymbol{a}^\top \boldsymbol{x}|. \tag{22}$$

A simple calculation leads to $1/\delta_0 \lesssim 1/\sqrt{\beta}$. Combining (21) and (22), we can obtain that $G(\boldsymbol{a}^\top \boldsymbol{z}, \boldsymbol{a}^\top \boldsymbol{x}, \boldsymbol{a}^\top \boldsymbol{v})$ satisfies the Lipschitz type condition with respect to $\boldsymbol{z}$ in Lemma 2.1 with subgaussian norm $\eta = O(1/\beta^{2.5})$. Applying the same arguments to $\boldsymbol{v}$ and recognizing that $\psi_2(t)$ is a Lipschitz function with Lipschitz norm $O(1)$, we can obtain $G(\boldsymbol{a}^\top \boldsymbol{z}, \boldsymbol{a}^\top \boldsymbol{x}, \boldsymbol{a}^\top \boldsymbol{v})$ satisfies the Lipschitz type condition with respect to $\boldsymbol{v}$ as in Lemma 2.1 with subgaussian norm $\eta = O(1/\beta)$. This completes the proof. ■

6. Appendix: auxiliary lemmas

Lemma 6.1 *([40], Theorem 2.8.1). Let $g(s,t)$ be a real valued function such that $g(\boldsymbol{a}_i^\top \boldsymbol{z}, \boldsymbol{a}_i^\top \boldsymbol{x})$ is subexponential with subexponential norm $\|g(\boldsymbol{a}_i^\top \boldsymbol{z}, \boldsymbol{a}_i^\top \boldsymbol{x})\|_{\Psi_1} \le \tau$. Then for any $\varepsilon > 0$ we have*

$$\left|\frac{1}{m}\sum_{i=1}^{m} g(\boldsymbol{a}_i^\top \boldsymbol{z}, \boldsymbol{a}_i^\top \boldsymbol{x}) - \mathbb{E}[g(\boldsymbol{a}_1^\top \boldsymbol{z}, \boldsymbol{a}_1^\top \boldsymbol{x})]\right| \le \varepsilon \tag{23}$$

with probability at least $1 - 2\exp(-cm\min(\varepsilon^2/\tau^2, \varepsilon/\tau))$, where $c > 0$ is a universal constant.

Lemma 6.2. *Let $\Psi(u,v) = \frac{1}{2}\left(\gamma\left(\frac{u}{v}\right) - 1\right)^2 v^2$ as defined in (9). Then the derivative $\Psi_u(u,v)$ of $\Psi(u,v)$ satisfies*

$$|\Psi_u(u,v)| \le |u| + |v|, \quad \Psi_u(u,v)u \ge u^2 - |uv|,$$

and

$$|\Psi_u(u_1,v) - \Psi_u(u_2,v)| \le \max(1, |2 - 1/\beta|) \cdot |u_1 - u_2|.$$

Proof. The boundedness and Lipschitz property of Ψ_u are easy to check and we only prove the bound

$$\Psi_u(u,v)u \ge u^2 - |uv|. \tag{24}$$

Recall the expression (10) of $\Psi_u(u,v)$. It immediately gives

$$\frac{\Psi_u(u,v)u}{v^2} = \begin{cases} \left(\frac{u}{v}\right)^2 - \left|\frac{u}{v}\right|, & |u| > \beta|v|; \\ \frac{1}{2\beta^2}\cdot\left(\frac{u}{v}\right)^4 + \left(\frac{1}{2} - \frac{1}{\beta}\right)\left(\frac{u}{v}\right)^2, & |u| \le \beta|v|. \end{cases}$$

Thus, to prove (24) it suffices to show

$$\frac{1}{2\beta^2}t^4 + \left(\frac{1}{2} - \frac{1}{\beta}\right)t^2 \ge t^2 - |t|$$

for all $|t| \le \beta$. Due to the symmetry, we only need to consider the case $0 \le t \le \beta$. Let

$$h(t) = t^3 - (\beta^2 + 2\beta)t + 2\beta^2.$$

It is easy to check that $h(t)$ is a decreasing function for $0 \le t \le \beta$. Note that $h(\beta) = 0$. It then gives $h(t) \ge 0$ for all $0 \le t \le \beta$. This completes the proof. ■

Lemma 6.3. *Under the assumption (A3) in Section 5.1, let $G(\lambda) := \mathbb{E}[g(U,V)\mathbb{1}_A]$ where $g(t,s)$ is continuous. Then*

$$\frac{dG}{d\lambda} = \frac{1}{2\pi\tau}\int_0^\infty \left(g(-\lambda v, v) + g(\lambda v, -v)\right) v e^{-\frac{1}{2}\mu_+^2 v^2} dv$$
$$+ \frac{1}{2\pi\tau}\int_0^\infty \left(g(\lambda v, v) + g(-\lambda v, -v)\right) v e^{-\frac{1}{2}\mu_-^2 v^2} dv.$$

Proof. Observe that $U = \sigma V + \tau W$. Then the condition $|U| \leq \lambda |V|$ is equivalent to

$$A = \left\{ \tau^{-1}(-\lambda - \sigma \operatorname{sgn}(V))|V| \leq W \leq \tau^{-1}(\lambda - \sigma \operatorname{sgn}(V))|V| \right\}.$$

From the definition, we have

$$\begin{aligned} G(\lambda) = \mathbb{E}\left[g(U,V)\mathbb{1}_A\right] &= \frac{1}{2\pi} \int \int\limits_{|\sigma v + \tau w| \leq \lambda |v|} g(\sigma v + \tau w, v) e^{-\frac{1}{2}(v^2+w^2)} dw dv \\ &= \frac{1}{2\pi} \int\limits_0^\infty \int\limits_{-(\frac{\lambda}{\tau}+\frac{\sigma}{\tau})v}^{(\frac{\lambda}{\tau}-\frac{\sigma}{\tau})v} g(\sigma v + \tau w, v) e^{-\frac{1}{2}(v^2+w^2)} dw dv \\ &\quad + \frac{1}{2\pi} \int\limits_{-\infty}^0 \int\limits_{(\frac{\lambda}{\tau}-\frac{\sigma}{\tau})v}^{-(\frac{\lambda}{\tau}+\frac{\sigma}{\tau})v} g(\sigma v + \tau w, v) e^{-\frac{1}{2}(v^2+w^2)} dw dv. \end{aligned}$$

It then gives that

$$\begin{aligned} G'(\lambda) &= \frac{1}{2\pi\tau} \int\limits_0^\infty g(\lambda v, v) v e^{-\frac{1}{2}\mu_-^2 v^2} dv + \frac{1}{2\pi\tau} \int\limits_0^\infty g(-\lambda v, v) v e^{-\frac{1}{2}\mu_+^2 v^2} dv \\ &\quad - \frac{1}{2\pi\tau} \int\limits_{-\infty}^0 g(-\lambda v, v) v e^{-\frac{1}{2}\mu_+^2 v^2} dv - \frac{1}{2\pi\tau} \int\limits_{-\infty}^0 g(\lambda v, v) v e^{-\frac{1}{2}\mu_-^2 v^2} dv \\ &= \frac{1}{2\pi\tau} \int\limits_0^\infty \left(g(-\lambda v, v) + g(\lambda v, -v)\right) v e^{-\frac{1}{2}\mu_+^2 v^2} dv \\ &\quad + \frac{1}{2\pi\tau} \int\limits_0^\infty \left(g(\lambda v, v) + g(-\lambda v, -v)\right) v e^{-\frac{1}{2}\mu_-^2 v^2} dv. \quad \blacksquare \end{aligned}$$

Corollary 6.4. *Assume that $g(t,s) = |t|^p |s|^q$ in Proposition 6.3 where $p + q \geq 0$. Then*

$$G'(\lambda) = \frac{\lambda^p}{\pi\tau} \left(\mu_-^{-(p+q+2)} + \mu_+^{-(p+q+2)} \right) \int\limits_0^\infty t^{p+q+1} e^{-\frac{1}{2}t^2} dt.$$

In particular, if $p + q = 2$ then $G'(\lambda) = \frac{2\lambda^p}{\pi\tau}(\mu_-^{-4} + \mu_+^{-4})$.

Proof. This is a straightforward application of Proposition 6.3. Observe that for $p + q = 2$ the integral $\int_0^\infty t^3 e^{-\frac{1}{2}t^2} dt = 2$. $\blacksquare$

Corollary 6.5. *Assume that $g(t,s) = \operatorname{sgn}(ts)|t|^p |s|^q$ in Lemma 6.3 where $p + q \geq 0$. Then*

$$G'(\lambda) = \frac{\lambda^p}{\pi\tau} \left(\mu_-^{-(p+q+2)} - \mu_+^{-(p+q+2)} \right) \int\limits_0^\infty t^{p+q+1} e^{-\frac{1}{2}t^2} dt.$$

Hence $G(\lambda) \geq 0$. In particular, if $p + q = 2$ then $G'(\lambda) = \frac{2\lambda^p}{\pi\tau}(\mu_-^{-4} - \mu_+^{-4})$.

Proof. Same as the previous corollary. ■

Lemma 6.6. *Let $\boldsymbol{a} \sim \mathcal{N}(0, I_n)$ be a standard Gaussian vector in $\mathbb{R}^n$. Then*

$$\mathbb{E}[|\boldsymbol{a}^\top \boldsymbol{z}||\boldsymbol{a}^\top \boldsymbol{x}|] = \frac{2}{\pi}\left(\tau + \sigma \arctan\frac{\sigma}{\tau}\right)\|\boldsymbol{z}\|\|\boldsymbol{x}\|,$$
$$\mathbb{E}[\operatorname{sgn}((\boldsymbol{a}^\top \boldsymbol{z})(\boldsymbol{a}^\top \boldsymbol{x}))|\boldsymbol{a}^\top \boldsymbol{x}|^2)] = \frac{2}{\pi}\left(\tau\sigma + \arctan\frac{\sigma}{\tau}\right)\|\boldsymbol{x}\|^2,$$

where $\sigma = \sigma(\boldsymbol{z}) := \langle \boldsymbol{z}, \boldsymbol{x}\rangle / \|\boldsymbol{z}\|\|\boldsymbol{x}\|$ and $\tau = \tau(\boldsymbol{z}) := \sqrt{1-\sigma^2}$.

Proof. Without loss of generality, we assume $\|\boldsymbol{z}\| = \|\boldsymbol{x}\| = 1$. For the expectation $\mathbb{E}[|\boldsymbol{a}^\top \boldsymbol{z}||\boldsymbol{a}^\top \boldsymbol{x}|]$, let $\sigma = \cos\alpha$ for some $\alpha \in [0, 2\pi)$. Then we have

$$\begin{aligned}
\mathbb{E}[|\boldsymbol{a}^\top \boldsymbol{z}||\boldsymbol{a}^\top \boldsymbol{x}|] &= \frac{1}{2\pi}\int_{-\infty}^{\infty}\int_{-\infty}^{\infty} |v(\sigma v + \tau w)| \cdot e^{-\frac{1}{2}(v^2+w^2)} dw dv \\
&= \frac{1}{2\pi}\int_{0}^{2\pi}\int_{0}^{\infty} r^3 |\sin\theta| \cdot |\sigma\sin\theta + \tau\cos\theta| \cdot e^{-\frac{1}{2}r^2} dr d\theta \\
&= \frac{1}{\pi}\int_{0}^{2\pi} |\sin\theta \sin(\theta+\alpha)| d\theta \\
&= \frac{2}{\pi}\left(\sin\alpha + (\frac{\pi}{2} - \alpha)\cos\alpha\right) \\
&= \frac{2}{\pi}\left(\tau + \sigma\arctan\frac{\sigma}{\tau}\right).
\end{aligned}$$

Similarly,

$$\begin{aligned}
\mathbb{E}[\operatorname{sgn}((\boldsymbol{a}^\top \boldsymbol{z})(\boldsymbol{a}^\top \boldsymbol{x}))|\boldsymbol{a}^\top \boldsymbol{x}|^2)] &= \frac{1}{2\pi}\int_{-\infty}^{\infty}\int_{-\infty}^{\infty} \operatorname{sgn}(\sigma v^2 + \tau v w) \cdot v^2 \cdot e^{-\frac{1}{2}(v^2+w^2)} dw dv \\
&= \frac{1}{\pi}\int_{0}^{2\pi} \operatorname{sgn}\left(\sin\theta\sin(\theta+\alpha)\right)\sin^2\theta d\theta \\
&= \frac{2}{\pi}\int_{0}^{\pi-\alpha} \sin^2\theta d\theta - \frac{2}{\pi}\int_{\pi-\alpha}^{\pi} \sin^2\theta d\theta \\
&= \frac{2}{\pi}\left(\sin(2\alpha) + \frac{\pi}{2} - \alpha\right) \\
&= \frac{2}{\pi}\left(\tau\sigma + \arctan\frac{\sigma}{\tau}\right).
\end{aligned}$$

This completes the proof. ■

References

[1] A. Agarwal, A. Anandkumar, P. Netrapalli, Exact recovery of sparsely used overcomplete dictionaries, Stat 1050 (2013) 8–39.

[2] A. Anandkumar, P. Jain, Y. Shi, U.N. Niranjan, Tensor vs. matrix methods: robust tensor decomposition under block sparse perturbations, in: Artificial Intelligence and Statistics, 2016, pp. 268–276.
[3] S. Arora, R. Ge, A. Moitra, New algorithms for learning incoherent and overcomplete dictionaries, in: Conference on Learning Theory, 2014, pp. 779–806.
[4] B. Balan, On signal reconstruction from its spectrogram, in: 44th Annual Conference on Information Sciences and Systems (CISS), IEEE, 2010, pp. 1–4.
[5] B. Balan, P. Casazza, D. Edidin, On signal reconstruction without phase, Appl. Comput. Harmon. Anal. 20 (3) (2006) 345–356.
[6] T. Bendory, Y.C. Eldar, N. Boumal, Non-convex phase retrieval from STFT measurements, IEEE Trans. Inf. Theory 64 (1) (2017) 467–484.
[7] S. Bhojanapalli, N. Behnam, N. Srebro, Global optimality of local search for low rank matrix recovery, in: Advances in Neural Information Processing Systems, 2016, pp. 3873–3881.
[8] E.J. Candès, X. Li, Solving quadratic equations via PhaseLift when there are about as many equations as unknowns, Found. Comput. Math. 14 (5) (2014) 1017–1026.
[9] E.J. Candès, X. Li, M. Soltanolkotabi, Phase retrieval via Wirtinger flow: theory and algorithms, IEEE Trans. Inf. Theory 61 (4) (2015) 1985–2007.
[10] E.J. Candès, T. Strohmer, V. Voroninski, PhaseLift: exact and stable signal recovery from magnitude measurements via convex programming, Commun. Pure Appl. Math. 66 (8) (2013) 1241–1274.
[11] Y. Chen, E.J. Candès, Solving random quadratic systems of equations is nearly as easy as solving linear systems, Commun. Pure Appl. Math. 70 (5) (2017) 822–883.
[12] A. Chai, M. Moscoso, G. Papanicolaou, Array imaging using intensity-only measurements, Inverse Probl. 27 (1) (2010) 015005.
[13] A. Conca, D. Edidin, M. Hering, C. Vinzant, An algebraic characterization of injectivity in phase retrieval, Appl. Comput. Harmon. Anal. 38 (2) (2015) 346–356.
[14] J.C. Dainty, J.R. Fienup, Phase retrieval and image reconstruction for astronomy, Image Recovery: Theory and Application 231 (1987) 275.
[15] S.S. Du, J.D. Lee, On the power of over-parametrization in neural networks with quadratic activation, in: International Conference on Machine Learning, 2018, pp. 1329–1338.
[16] S.S. Du, C. Jin, J.D. Lee, M.I. Jordan, Gradient descent can take exponential time to escape saddle points, in: Advances in Neural Information Processing Systems, 2017, pp. 1067–1077.
[17] J.R. Fienup, Phase retrieval algorithms: a comparison, Appl. Opt. 21 (15) (1982) 2758–2769.
[18] B. Gao, X. Sun, Y. Wang, Z. Xu, Perturbed amplitude flow for phase retrieval, IEEE Trans. Signal Process. 68 (2020) 5427–5440.
[19] B. Gao, Z. Xu, Phaseless recovery using the Gauss–Newton method, IEEE Trans. Signal Process. 65 (22) (2017) 5885–5896.
[20] R. Ge, F. Huang, C. Jin, Y. Yuan, Escaping from saddle points—online stochastic gradient for tensor decomposition, in: Conference on Learning Theory, 2015, pp. 797–842.
[21] R. Ge, J. Lee, C. Jin, T. Ma, Matrix completion has no spurious local minimum, in: Advances in Neural Information Processing Systems, 2016, pp. 2973–2981.
[22] R.W. Gerchberg, A practical algorithm for the determination of phase from image and diffraction plane pictures, Optik 35 (1972) 237–246.
[23] R.W. Harrison, Phase problem in crystallography, JOSA A 10 (5) (1993) 1046–1055.
[24] M. Huang, Y. Wang, Linear convergence of randomized Kaczmarz method for solving complex-valued phaseless equations [Online]. Available: http://arxiv.org/abs/2109.11811, 2021.
[25] M. Huang, Z. Xu, Solving systems of quadratic equations via exponential-type gradient descent algorithm, J. Comput. Math. 38 (4) (2020).
[26] K. Jaganathan, Y.C. Eldar, B. Hassibi, Phase retrieval: an overview of recent developments, in: Optical Compressive Imaging, 2016, pp. 279–312.
[27] C. Jin, R. Ge, P. Netrapalli, S.M. Kakade, M.I. Jordan, How to escape saddle points efficiently, in: Proceedings of the 34th International Conference on Machine Learning, vol. 70, 2017, pp. 1724–1732.
[28] C. Jin, P. Netrapalli, M.I. Jordan, Accelerated gradient descent escapes saddle points faster than gradient descent [Online]. Available: http://arxiv.org/abs/1711.10456, 2017.
[29] K. Lee, Y. Li, M. Junge, Y. Bresler, Blind recovery of sparse signals from subsampled convolution, IEEE Trans. Inf. Theory 63 (2) (2016) 802–821.
[30] Z. Li, J.F. Cai, K. Wei, Towards the optimal construction of a loss function without spurious local minima for solving quadratic equations, IEEE Trans. Inf. Theory 66 (5) (2020) 3242–3260.
[31] J. Miao, T. Ishikawa, Q. Shen, T. Earnest, Extending x-ray crystallography to allow the imaging of noncrystalline materials, cells, and single protein complexes, Annu. Rev. Phys. Chem. 59 (2008) 387–410.
[32] R.P. Millane, Phase retrieval in crystallography and optics, J. Opt. Soc. Am. A 7 (3) (1990) 394–411.
[33] P. Netrapalli, P. Jain, S. Sanghavi, Phase retrieval using alternating minimization, IEEE Trans. Signal Process. 63 (18) (2015) 4814–4826.
[34] D. Park, A. Kyrillidis, C. Caramanis, Non-square matrix sensing without spurious local minima via the Burer-Monteiro approach [Online]. Available: http://arxiv.org/abs/1609.03240, 2016.
[35] H. Sahinoglou, S.D. Cabrera, On phase retrieval of finite-length sequences using the initial time sample, IEEE Trans. Circuits Syst. 38 (8) (1991) 954–958.
[36] Y. Shechtman, Y.C. Eldar, O. Cohen, H.N. Chapman, J. Miao, M. Segev, Phase retrieval with application to optical imaging: a contemporary overview, IEEE Signal Process. Mag. 32 (3) (2015) 87–109.
[37] M. Soltanolkotabi, A. Javanmard, J.D. Lee, Theoretical insights into the optimization landscape of over-parameterized shallow neural networks, IEEE Trans. Inf. Theory 65 (2) (2018) 742–769.

[38] J. Sun, Q. Qu, J. Wright, A geometric analysis of phase retrieval, Found. Comput. Math. 18 (5) (2018) 1131–1198.

[39] J. Sun, Q. Qu, J. Wright, Complete dictionary recovery over the sphere I: overview and the geometric picture, IEEE Trans. Inf. Theory 63 (2) (2016) 853–884.

[40] R. Vershynin, High-Dimensional Probability: An Introduction with Applications in Data Science, Cambridge Univ. Press, U.K., 2018.

[41] I. Waldspurger, Phase retrieval with random Gaussian sensing vectors by alternating projections, IEEE Trans. Inf. Theory 64 (5) (2018) 3301–3312.

[42] I. Waldspurger, A. d'Aspremont, S. Mallat, Phase recovery, maxcut and complex semidefinite programming, Math. Program. 149 (1–2) (2015) 47–81.

[43] A. Walther, The question of phase retrieval in optics, J. Mod. Opt. 10 (1) (1963) 41–49.

[44] G. Wang, G.B. Giannakis, Y.C. Eldar, Solving systems of random quadratic equations via truncated amplitude flow, IEEE Trans. Inf. Theory 64 (2) (2018) 773–794.

[45] L.H. Yeh, et al., Experimental robustness of Fourier ptychography phase retrieval algorithms, Opt. Express 23 (26) (2015) 33214–33240.

[46] H. Zhang, Y. Zhou, Y. Liang, Y. Chi, A nonconvex approach for phase retrieval: reshaped Wirtinger flow and incremental algorithms, J. Mach. Learn. Res. 18 (1) (2017) 5164–5198.